Am J Transl Res 2025;17(10):8243-8264
www.ajtr.org /ISSN:1943-8141/AJTR0161837

Original Article

PLXND1 from the Plexins family is a prognostic factor promoting colon cancer invasion and metastasis

Wenxing Chen[1*], Liqun Guo[2*], Zeen Wang[1], Ziwei Wang[1], Xinglong Dai[1]

[1]*Gastrointestinal Surgical Unit, The First Affiliated Hospital of Chongqing Medical University, Chongqing, PR China;* [2]*Business School of Guilin University of Technology, Guilin, Guangxi Zhuang Autonomous Region, PR China.* [*]*Equal contributors.*

Received November 7, 2024; Accepted September 11, 2025; Epub October 15, 2025; Published October 30, 2025

Abstract: Objectives: To elucidate the expression profile, immune infiltration, prognostic value, and role of Plexins in Colonic Adenocarcinoma (COAD). Methods: The levels of the Plexins family members in COAD were verified, and their effect on clinical characteristics, immune infiltration, and prognosis were explored by The Cancer Genome Atlas (TCGA), Expression Atlas, and Human Protein Atlas (HPA) databases. The core molecule of Plexins, PLXND1, was screened and validated in COAD by qRT-PCR, immunohistochemistry, wound healing, transwell, immunofluorescence, western blotting, immunoprecipitation, and animal experiments. Results: The PLXNA1/PLXNA3/PLXNA4/PLXNB1/PLXND1 levels were increased in COAD samples, whereas the levels of PLXNA2/PLXNB3/PLXNC1 were reduced. High PLXNA3/PLXNA4/PLXNB3/PLXND1 levels were related to the higher lymph node stage of COAD patients. Most Plexin levels were prominently associated with the infiltration of T cell regulators, macrophage M0, and eosinophils in COAD samples. High PLXNA3/PLXNB3/PLXND1 levels were interrelated with poor overall survival of COAD patients, and PLXND1 was a novel independent prognostic indicator. Furthermore, the PLXND1-associated differential molecular regulatory networks were analyzed, and the expression of PLXND1 was markedly increased in COAD tissues and lymph node-positive COAD patients. Mechanistically, PLXND1 promoted COAD cell invasion, metastasis, and epithelial-mesenchymal transition (EMT) ability by binding and modulating Notch3 signaling. Conclusions: Data mining revealed the crucial roles of the Plexin family in COAD, especially in clinical indicators, immune infiltration, and prognosis of COAD patients. PLXND1, as an independent prognostic biomarker, enabled COAD cell invasion, metastasis and EMT by binding and modulating Notch3 signaling.

Keywords: Plexins, COAD, immune, prognosis, PLXND1, metastasis

Introduction

Colon adenocarcinoma (COAD) is the third most common malignancy in the world, and advanced COAD is the second leading cause of cancer death [1]. Despite continuous improvement in diagnostic and therapeutic strategies, rapid proliferative capacity, lymphatic/hematogenous metastasis, and direct invasive behavior are key factors contributing to the poor prognosis of COAD patients. Radical surgery, adjuvant therapy, preoperative neoadjuvant chemotherapy, molecularly targeted agents (anti-VEGF, anti-EGFR), and immunotherapy have emerged as effective treatment strategies [2]. Although numerous studies have been conducted on the occurrence and progression of COAD, the etiology and pathogenesis of COAD remain to be elucidated [3]. Genomic disorders have been reported in the literature by The Cancer Genome Atlas (TCGA), which includes simple nucleotide variants, copy number variants, transcriptome profiles, DNA methylation, sequencing reads, and clinical data from various cancers. To further investigate the mechanisms of COAD progression and therapeutic effects, it is necessary to explore more potential molecular targets or gene families for patients with COAD using published or publicly available genomic data.

Plexins comprise nine single-pass receptors initially described in the nervous system. The Plexins family contains plexins type A (PLXNA1-A4), plexins type B (PLXNB1-B3), plexin type C (PLXNC1), and plexin type D (PLXND1)

https://doi.org/10.62347/NAGL6201

[4, 5]. Among the extracellular domains of Plexins, the semaphoring domain acts as an autoinhibitory structural domain when the receptor is substantially inactive. Upon binding to semaphorin, a conformational change releases the inhibitory effect. Once the GTPase activating (GAP) domain is changed or mutated, the developmental roles of PLXNB1 and PLXND1 are lost, indicating that it plays a vital role in Plexin-mediated signaling [6, 7]. Some studies have reported that the semaphorin/Plexins complexes control most biological processes, but an imbalance of Plexins has also been associated with various pathological conditions. Also, mechanisms by which PLXNC1 inhibits excessive atypical inflammasome activity and provides a new potential target for the treatment of sepsis [8]. Elevated PLXNA1 expression facilitated prostate cancer proliferation under enzalutamide treatment due to AKT signaling activation [9]. The pro-proliferative effects of plexin-A2 are mediated by FARP2 and FYN and by the GAP domain located in the intracellular domain of plexin-A2 in tumors from glioblastoma-derived cells [10]. PLXNB3 is required for hypoxia-induced MET/SRC/focal adhesion kinase (FAK) and MET/SRC/STAT3/NANOG signaling as well as hypoxia-induced breast cancer cell migration, invasion, and cancer stem cell specification [11]. However, the functions and mechanisms of the Plexin family are not yet fully known in multiple cancers, and their role in COAD patients is uncertain.

In this study, we present a comprehensive analysis of Plexin expression, enrichment analysis, immune cell infiltration, and correlation with the prognosis of COAD patients from the latest public databases (including TCGA, Human Protein Atlas (HPA), Expression Atlas). The data demonstrated that the levels of some Plexins (PLXNA3, PLXNA4, PLXNB3, PLXND1) were imbalanced in COAD, and this imbalance was more dramatic in lymph node metastasis. The levels of most Plexins correlated with immune cell levels, immune subtypes, and stromal cell infiltration in the COAD microenvironment. High levels of PLXNA3, PLXNB3, and PLXND1 were related to poor survival period of COAD patients, and PLXND1 was an independent prognostic factor. Based on this, we screened the Plexins family and found that only PLXND1 played a role in multiple aspects of COAD. Then, PLXND1 was screened and subjected to molecular and signaling pathway analyses and functional experiments. Further functional experiments revealed that the PLXND1 promoted invasion and metastasis of COAD by binding and modulating Notch3 signaling. These data explain the role of Plexins family in COAD progression may help develop new therapeutic targets.

Materials and methods

TCGA data of the Plexins family

HTSeq-FPKM data for the COAD cohort were obtained and downloaded from the Genomic Data Commons Data Portal (GDC) of the TCGA using Perl 5.26 software, including 473 primary COAD samples and 41 normal samples. After excluding COAD patients with incomplete or repeated clinical data, the complete data included clinical information of 452 COAD patients, including age, gender, clinical stage, metastasis (M) stage, tumor (T) stage, lymph node (N) stage, and survival time. We obtained 35 cases of pathologically diagnosed COAD tissues and normal adjacent tissues from April to October 2020 from the First Hospital of Chongqing Medical University. The COAD patients voluntarily signed informed consent forms. The study was authorized by the First Affiliated Hospital Ethics Committee of Chongqing Medical University.

Expression levels of Plexins in COAD tissues and cells

The levels of Plexins in multiple cancers were analyzed from TCGA data using the ggpubr package. The corrplot and circlize packages were utilized to examine the correlations of Plexin molecules in COAD samples. The levels of Plexins in COAD and normal samples were gained and calculated using the limma and beeswarm packages. We obtained the levels of Plexins in COAD cells using the Expression Atlas database [12]. In addition, the association between clinicopathologic data (M stage, N stage, Tumor Node Metastasis (TNM) stage, T stage) and Plexins family expression was analyzed through logistic regression and the Wilcoxon signed-rank test, respectively.

Gene set enrichment analysis (GSEA)

GSEA (Version 4.3.0) was used to identify gene clusters and pathways related to the expres-

sion of Plexins in TCGA-COAD samples. The annotated gene set file c2.cp.kegg.v7.4.symbols.gmt was taken as a reference (from the MSigDB database). Then, enrichment analysis was employed using 1,000 permutations of random combinations and a false discovery rate (FDR) <0.05 as the criterion for validating markedly enriched genes. The gene sets were categorized into low- and high-expression Plexins according to the expression levels of median Plexins, and the roles of Plexins in COAD were evaluated.

Correlation analysis between Plexins and immune cell infiltration in COAD

CIBERSORT validated the composition of immune cells in tumors by using gene expression values corresponding to the "signature matrix" of 547 genes [13, 14]. The expression levels were normalized, and the CIBERSORT algorithm was run to discover the 22 kinds of different immune cells among 473 COAD samples using R software. A heatmap and bar chart revealed the immune cell composition of each sample; correlations between the abundance of immune cells were detected using the pheatmap package. To confirm the significance of the above data, we investigated the immune cells associated with Plexins in COAD samples using two methods. 1) Difference method: COAD samples were divided into high- or low-expression groups according to the median expression of Plexins, and the differences in tumor-infiltrating immune cells were observed. 2) Correlation method: The Pearson correlation coefficient was used to detect the correlation between the expression of Plexins and immune cells. Scatter plots of the correlation between Plexin's expression and immune cells were calculated and plotted using Spearman's correlation and estimated statistics. Tumor purity, ImmuneScore, StromalScore, and ESTIMATEScore were calculated and analyzed for COAD samples using the ESTIMATE package.

Survival analysis of Plexins in COAD

The following methods were used to explore the prognostic value of Plexins: 1) COAD patients were divided into two groups according to the median expression levels of the specific Plexins. The survival of COAD patients was analyzed using the Kaplan-Meier analysis and log-rank test. 2) The relationships between Plexin expression, survival, and clinical data of COAD patients were analyzed using univariate Cox regression analysis. 3) The prognostic roles of Plexins were calculated and evaluated using multivariate Cox regression analysis and controlling for the clinical parameters in step 2 above. 4) We developed a nomogram model to predict and calculate the 1-, 3-, and 5-year survival rates of patients with COAD. Every factor corresponds to a score in the first row regarding the nomogram design. Calibration curves were created to assess the predictive power of the nomogram.

Clinical value of targeted drug screening

A risk score was calculated for each COAD patient and then divided into high- and low-risk groups based on the median risk score. The drug sensitivities were assessed in COAD patients with different risk groups using the limma, ggpubr, and pRRophetic packages, which predict 50% inhibitory concentration (IC_{50}) of common drugs for COAD. Subsequently, we determined drug sensitivities in different risk groups and screened for therapeutic agents that might affect COAD patient survival. Differences between groups were assessed using the Wilcoxon signed-rank test, with P<0.001 as the screening criterion.

HPA data analysis

The Human Pathology Atlas project (https://www.proteinatlas.org) comprises immunohistochemistry (IHC) data based on tissue microarray, including proteome analysis of 17 leading cancer types and 44 major normal tissue types [15]. This study utilized the Human Pathology Atlas to investigate the protein level of PLXND1 in COAD and normal tissues. Staining of intensity, quantity, location, and patient information in COAD tissues was available online.

Functional enrichment analysis

The inclusion criteria for identifying differentially expressed genes (DEGs) according to the expression level of PLXND1 were set to logFC >2 and adjusted to P<0.05. The Gene Ontology (GO) and Kyoto Encyclopedia of Genes and Genomes (KEGG) pathway were performed based on DEGs by the R packages "cluster-

Profiler", "limma", "enrichplot", "org.Hs.eg.db", "DOSE", and "ggplot2". The R packages "GOplot" and "digest" were used for cluster analysis. The GO analysis consisted of three categories: cellular components (CC), biological processes (BP), and molecular functions (MF). Based on the expression level of PLXND1, we further analyzed and viewed the important protein-protein interaction networks using Cytoscape software (version 3.10.1) [16]. KEGG pathways and GO terms with a *P*-value <0.05 were deemed to enrich functional annotations dramatically. We listed the top 30 KEGG pathways and 10 GO biological processes.

Sample collection

The 35 cases of pathologically diagnosed COAD tissues and matched normal adjacent tissues were obtained from March to December 2020 from the First Hospital of Chongqing Medical University. The COAD patients did not receive immunotherapy, targeted therapy, or chemotherapy before the surgical operation. Clinical data and histopathology of COAD patients were obtained from medical records and pathology reports. All patients voluntarily filled out an informed consent form. This study and collection of tissue samples were authorized and agreed on by the Ethics Committee of the First Affiliated Hospital of Chongqing Medical University.

Cell culture and transfection

HCT116, SW480, LOVO, HCT8, HT29, and SW620 were cultured in RPMI 1640 medium (GIBCO, USA) mixed with 10% qualified fetal bovine serum (FBS, VivaCell, New Zealand) at 37°C containing 5% CO_2. The cells were obtained and purchased from the Cell Bank of the Chinese Academy of Sciences (China). All PLXND1 interfering siRNAs were designed and synthesized from GenePharma (China). To construct the PLXND1 overexpression vector, the cDNA of PLXND1 into LV5 lentivirus was designed and synthesized by GenePharma. Then, the COAD cells were incubated with 2 μg/ml puromycin, and stably transfected cell lines were obtained. All oligonucleotides were treated in COAD cells using Lipofectamine 3000 (Invitrogen, China) according to the instructions of the manufacturer.

Quantitative reverse transcription-PCR (qRT-PCR)

Total RNAs from human COAD cells were extracted using TRIzol reagent according to the instructions of the manufacturer (Invitrogen, USA). The treated RNAs were performed to reverse transcription into cDNAs by the PrimeScript RT Reagent Kit (Takara, Japan). The TB Green Premix Ex Taq II was used for cDNA amplification according to the kit's protocols (Takara, Japan). The primers (Plexins family and GAPDH) were synthesized from Sangon Biotech (China) and listed in Supplementary Table 1. The $2^{-\Delta\Delta CT}$ method was utilized to normalize the molecules to internal control levels. The average amplified values of every molecule were repeated three times independently.

Wound healing assay

The treated cells were cultured with 5×10^5 cells per well in 6-well plates. When COAD cells had grown to 80% confluence, a 200 μl pipette was used to make a scratch of the same width. Images of wounds were observed using a microscope at 0 hours. Images were retaken 48 hours after the scratch at the same location for comparison. The rates of wound closure were calculated and compared.

Transwell assay

The invasion capacity was detected using the Matrigel matrix-coated 24-well Transwell chambers (Jet BioFil, China). The chamber cavity was filled with 200 μl of serum-free 1640 medium containing treated cells in suspension, and about 500 μl of medium, including 10% FBS, was mixed with the lower chambers for 24 h. The invaded lower membrane cells were washed, and 4% paraformaldehyde was used to fix the lower chambers. Then, the lower chambers of COAD cells were dyed with 0.1% Crystal Violet solution, and the invaded lower chambers were photographed and evaluated with a microscope and ImageJ software.

Western blotting (WB)

The total protein of the treated COAD cells was extracted using the RIPA lysis containing complete phosphatase as well as protease inhibitors (Beyotime, China). The BCA kits were uti-

lized to adjust the protein concentration similarly (Beyotime, China). We employed the 10% SDS-PAGE to separate the protein on the gel and transferred the protein to PVDF membranes (Millipore, USA). Then, the proteins of membranes were blocked using 5% non-fat milk powder for 1 hour and incubated with the corresponding antibody at 4°C overnight. The above membranes were washed with TBST solution and mixed with the secondary antibody for 1 hour. Then, bands of samples were visualized and developed by the Ultrasensitive ECL WB Substrate (ZEN BIO, China). Primary antibodies were PLXND1, Notch3, E-cadherin, Vimentin, and β-actin, which were obtained from Abcam (UK) or Proteintech (China).

Immunohistochemistry (IHC)

The sections of colon carcinoma/normal tissues were deparaffinized and rehydrated. After antigen retrieval, these sections were incubated with specific primary antibodies overnight at 4°C, including the PLXND1 (Abcam). Then, the HRP-conjugated secondary antibody was utilized to incubate for 1 hour, and the sections were stained with diamino aniline (DAB) and then counterstained with Mayer's hematoxylin. The marked positive tissues were captured and calculated using a fluorescence microscope (Carl Zeiss, Germany) and Image-Pro software.

Immunofluorescence (IF) staining

COAD cells overexpressing PLXND1 or transfected with siRNA were plated on 24-well plates. The 4% paraformaldehyde served to fix the cells on slides for 20 minutes, and the fixed cells were permeabilized using 0.5% Triton X-100 for 30 minutes. The washed cells were blocked with 5% bovine serum albumin for 1 hour. The specific primary antibodies, including E-cadherin, Vimentin, and Notch3, were incubated for 24 h at 4°C. Then, the fluorescent secondary antibody was stained for about 1 hour the next day. The cell nuclei were stained with DAPI for 15 minutes. The immunofluorescence staining was observed and photographed using a confocal fluorescence microscope (LSM800, Carl Zeiss, Germany).

Immunoprecipitation (IP)

Colon cancer cells were washed with PBS and then lysed with IP lysis buffer supplemented with protease inhibitors. Cells were centrifuged at 12,000× g for 10 minutes at 4°C to remove debris and retain the protein supernatant. The lysate was incubated with protein A/G agarose beads (20 μl) for 2 h at room temperature to reduce non-specific binding. The beads were then centrifuged (2,500× g, 1 min) and washed 3 times with lysis buffer. Subsequently, a primary antibody (5 μg per 500 μg of lysate) is added, and the beads were rotated at 4°C overnight. IgG from the same host species was used as a negative control. These bead complexes were resuspended in 1× loading buffer and boiled at 95°C for 5 min. The immunoprecipitates were obtained and analyzed by SDS-PAGE gel, stained with Coomassie Brilliant Blue, and western blotted.

Animal experiments

Four-week-old female BALB/c nude mice were preserved and divided into two groups (n=4/group). HCT8 cells stably transfected with the OE-PLXND1 vector or OE-NC were subcutaneously injected into the nude mice (2×10^6 cells per mouse). After several weeks, all mice were sacrificed. The tumor volume (length × width^2 × 0.5) was monitored every 7 days. The mice were euthanized after 30 days, and xenograft tumors were harvested for weight. Also, HCT8 cells transfected with the OE-PLXND1 vector or the OE-NC were injected into the tail vein of nude mice. The lungs of nude mice were dissected, and the metastatic tumor nodules were observed and calculated after 30 days. The animal experiments were approved by the Animal Care and Use Committee of Chongqing Medical University.

Statistical analysis

Data processing and statistical analyses were carried out using R software (v4.3.3), Perl (v5.26), SPSS (24.0), or GraphPad Prism (v8.2.1) software. The differences between the two groups were compared using the Student's t-test, and the differences among multiple groups were measured using one-way ANOVA. The *P*-values were calculated using the chi-square (χ^2), Student's t-test, or ANOVA. Survival rates of follow-up COAD patients were statistically analyzed using the Kaplan-Meier method and the log-rank test. Pearson's correlation coefficient analysis was used to analyze the correlations of Plexin members and the

related indicators. The quantitative data in graphs were expressed and counted as mean ± SD. *P*-values <0.05 were regarded as significant.

Results

Expression levels of the Plexins family

Plexins expression data (PLXNA1/2/3/4, PLXNB1/2/3, PLXNC1, PLXND1) were obtained from 23 different tumor samples (473 COAD samples and 41 normal samples) based on TCGA using Perl software. Plexin molecules displayed different expression levels in 23 tumor types (**Figure 1A**). For all cancer types, PLXNA1-A3, PLXNB1-B2, and PLXND1 showed relatively high expression levels with less heterogeneity, while PLXNA4, PLXNB3, and PLXNC1 were expressed at low levels with high heterogeneity. Differentially expressed Plexins were analyzed and visualized in COAD and normal samples using the beeswarm package (**Figure 1B**). The levels of PLXNA2, PLXNB3, and PLXNC1 were markedly down-regulated in COAD samples in comparison with normal samples, whereas PLXNA1, PLXNA3, PLXNA4, PLXNB1, and PLXND1 were prominently upregulated in COAD samples. The level of PLXNB2 displayed no significant difference between COAD samples and normal samples. Correlation analysis revealed a positive correlation between most Plexin molecules in the COAD samples (**Figure 1C**). PLXNA4 and PLXNC1 (Pearson correlation =0.64), PLXNA3 and PLXNB1 (Pearson correlation =0.62) showed a significant positive correlation, while PLXNC1 and PLXNB1 (Pearson correlation =-0.29) discovered a negative correlation. Then, the expression levels of Plexins varied in different colon cancer cells, such as PLXNB1, PLXNA3, PLXNA1, and PLXNB2 had higher expression levels, and PLXNA4 had lower expression levels (**Figure 1D**). These data suggest that Plexin members play crucial roles in COAD progression, but heterogeneity still exists.

Correlation analysis between TNM stage or pathways and the Plexins family

According to clinical stage, the expression levels of PLXNA3 (P=0.013) and PLXNB3 (P=0.003) continuously and gradually increased in each subgroup of the stage, while other Plexins were not significantly different (**Figure 2A**, **2B**). At the tumor (T) stage, the expression level of PLXNB3 (P=0.018) gradually increased in the T subgroup, but other members showed no statistical difference (**Figure 2C**). Multiple Plexin molecules exhibiting differential expression in COAD were dysregulated at the high node (N) stage, including PLXNA3, PLXNA4, PLXNB3, and PLXND1 (**Figure 2D-G**). For the metastatic (M) stage, PLXNA3 and PLXNB3 were increased in the M1 phase compared to the M0 phase, but the remaining Plexins showed no significant difference in the metastatic stage (**Figure 2H**, **2I**, Supplementary Figure 1). Next, to investigate the biological processes by which Plexins affect COAD carcinogenesis, GSEA analysis indicated that high expression levels of Plexins (excepting PLXNB1 and PLXNB2) were associated with “axon guidance”, “pathways in cancer”, “focal adhesion”, “T/B cell receptor”, “ECM receptor interaction”, and “regulation of actin cytoskeleton”. Low expression levels of Plexins (excepting PLXNA1 and PLXNB2) were related to “Parkinson’s”, “oxidative phosphorylation”, “Alzheimer’s disease”, and “Huntington’s disease” (**Figure 3**, Supplementary Table 1). These enrichment analyses revealed correlations between Plexins and key signaling sensors, suggesting that Plexins function in a cell-specific manner.

Correlation between Plexins and immune cell infiltration in COAD

The proportions of 22 kinds of tumor-infiltrating immune cells (TIICs) among 473 COAD samples were calculated and displayed based on the CIBERSORT algorithm. Results indicated that the ratios of TIICs were distinctly varied in each sample (Supplementary Figure 2A). T cell CD4 memory resting, Macrophages M0, M2, and other cells accounted for a high proportion of COAD samples. The infiltration levels of 22 kinds of TIICs showed a significant correlation in the COAD microenvironment. T cells CD4 memory activated, and T cells CD8 revealed a significant positive correlation (Pearson correlation =0.49), while Macrophages M0 and T cells CD8 showed a negative correlation (Pearson correlation =-0.47, Supplementary Figure 2B). Next, the different immune cell infiltration was screened according to the high- or low-expression of Plexins in COAD. Excluding PLXNC1, the infiltration levels of T cell regulators (Tregs) in the high-expressing

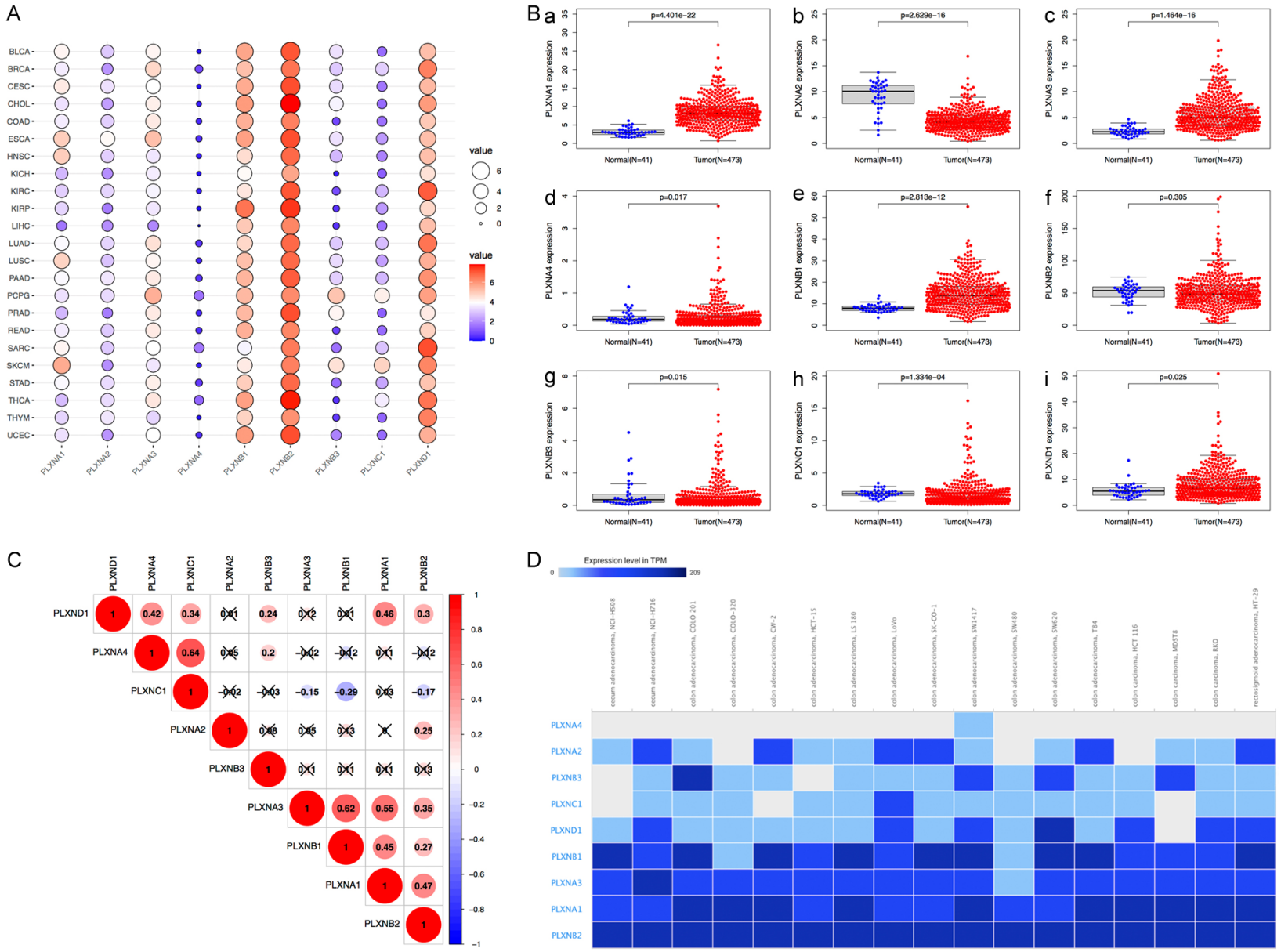
A
BLCA
BRCA
CESC
CHOL
COAD
ESCA
HNSC
KICH
KIRC
KIRP
LIHC
LUAD
LUSC
PAAD
PCPG
PRAD
READ
SARC
SKCM
STAD
THCA
THYM
UCEC
PLXNA1
PLXNA2
PLXNA3
PLXNA4
PLXNB1
PLXNB2
PLXNB3
PLXNC1
PLXND1
value
B
a
PLXNA1 expression
p=4.401e−22
b
PLXNA2 expression
p=2.629e−16
c
PLXNA3 expression
p=1.464e−16
d
PLXNA4 expression
p=0.017
e
PLXNB1 expression
p=2.813e−12
f
PLXNB2 expression
p=0.305
g
PLXNB3 expression
p=0.015
h
PLXNC1 expression
p=1.334e−04
i
PLXND1 expression
p=0.025
Normal(N=41)
Tumor(N=473)
C
PLXND1
PLXNA4
PLXNC1
PLXNA2
PLXNB3
PLXNA3
PLXNB1
PLXNA1
PLXNB2
D
Expression level in TPM
0
209
cecum adenocarcinoma, NCI-H508
cecum adenocarcinoma, NCI-H716
colon adenocarcinoma, COLO 201
colon adenocarcinoma, COLO-320
colon adenocarcinoma, CW-2
colon adenocarcinoma, HCT-15
colon adenocarcinoma, LS 180
colon adenocarcinoma, LoVo
colon adenocarcinoma, SK-CO-1
colon adenocarcinoma, SW1417
colon adenocarcinoma, SW480
colon adenocarcinoma, SW620
colon adenocarcinoma, T84
colon carcinoma, HCT 116
colon carcinoma, MDST8
colon carcinoma, RKO
rectosigmoid adenocarcinoma, HT-29

Figure 1. Expression levels of Plexin members. A: Expression levels of human Plexin members in 23 different cancer tissues. B: Expression levels of Plexin members in 473 COAD samples and 41 normal samples are represented by a beeswarm. Plexin members: a: PLXNA1; b: PLXNA2; c: PLXNA3; d: PLXNA4; e: PLXNB1; f: PLXNB2; g: PLXNB3; h: PLXNC1; i: PLXND1. C: Correlation of Plexin members in COAD samples. Red represents positive correlation, blue represents negative correlation, and X indicates no statistical difference. D: Expression Atlas data showed the expression levels of Plexin members in different COAD cells.

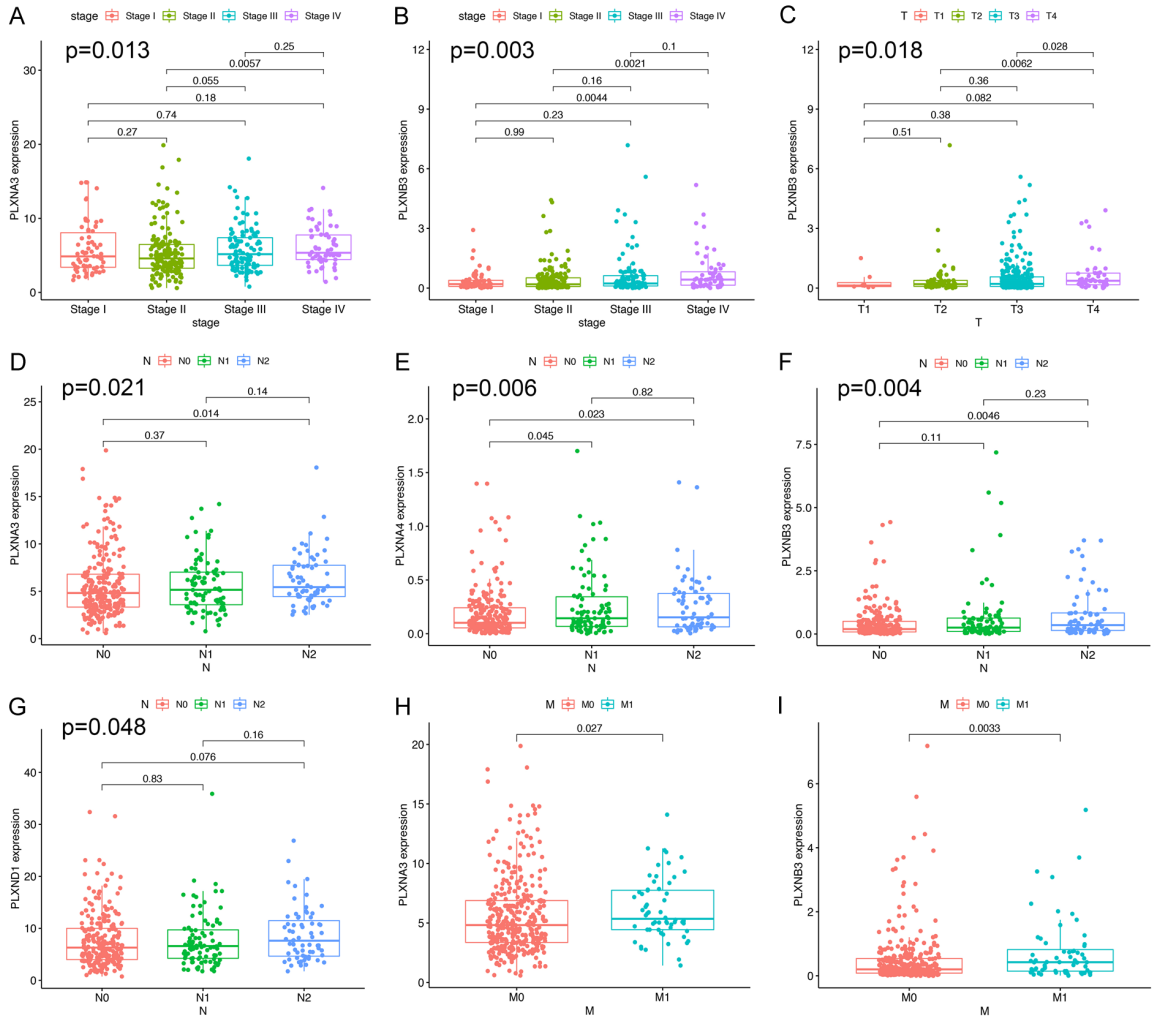

Figure 2. Correlation of Plexin expression with clinicopathologicstaging characteristics. A, B: Correlation analysis of clinical staging with Plexin expression in 452 COAD samples. C: Correlation analysis of T stage with Plexin expression in 452 COAD samples. D-G: Correlation analysis of N stage with Plexin expression in 452 COAD samples. H, I: Correlation analysis of M stage with Plexin expression in 452 COAD samples.

Plexins remarkably exceeded those in the low-expressing Plexins (**Figure 4**). Except for PLXNB2 and PLXNC1, the infiltration levels of Macrophages M0 were prominently increased in high-expressing Plexins compared with low-expressing Plexins. Except for PLXNA2, PLXNA4, and PLXNC1, the infiltration levels of eosinophils in high-expression Plexins were observably less than those in low-expression Plexins (**Figure 4**). Also, some other immune cells exhibited differential infiltration capacity between high- and low-expression Plexins in COAD (**Figure 4**). The correlation between Plexin expression levels and 22 types of TIICs was analyzed. An increased expression of Plexins (except PLXNC1) was positively correlated with the infiltration levels of Tregs in COAD patients (**Figure 5A**). With the increased expression of

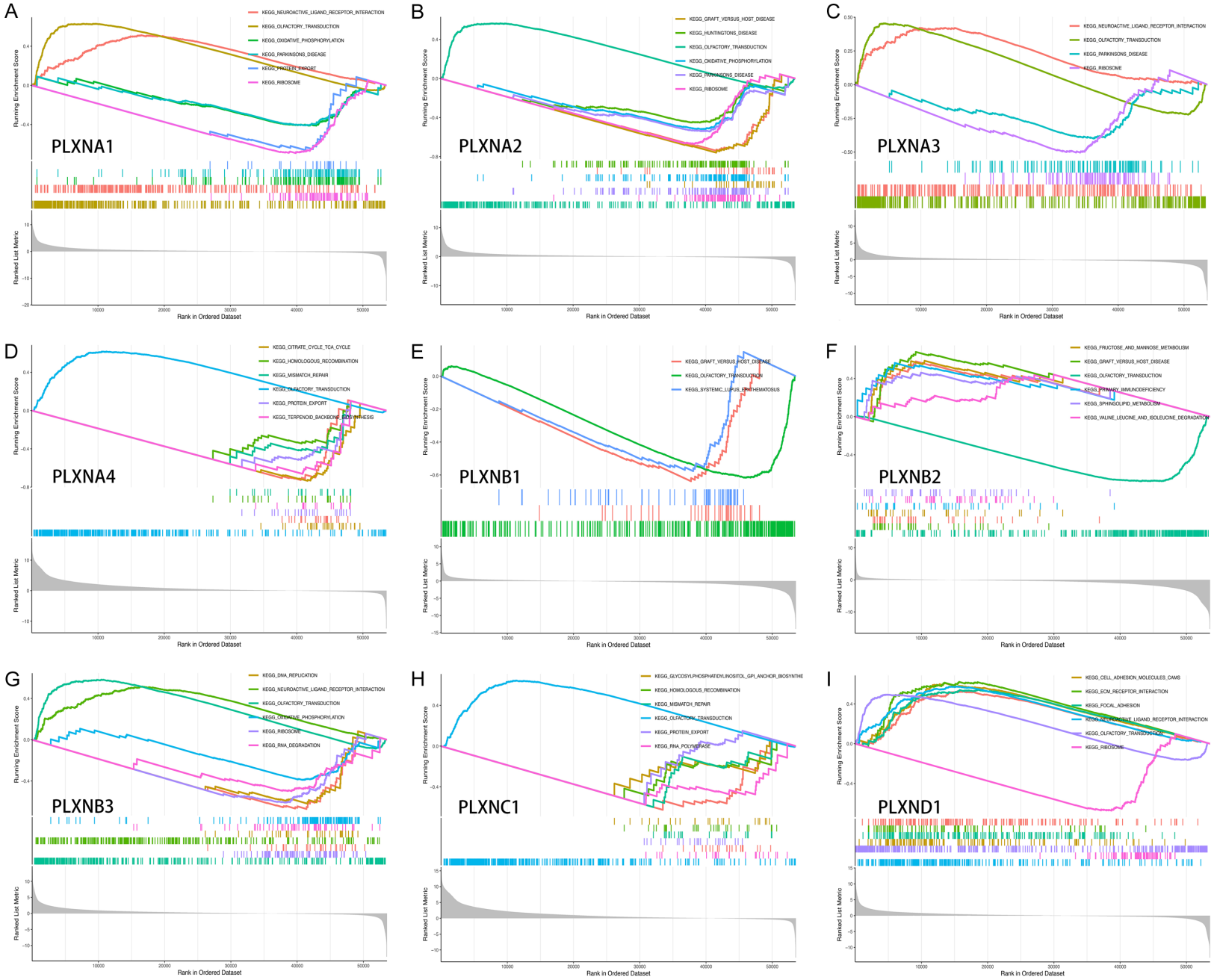
A
KEGG_NEUROACTIVE_LIGAND_RECEPTOR_INTERACTION
KEGG_OLFACTORY_TRANSDUCTION
KEGG_OXIDATIVE_PHOSPHORYLATION
KEGG_PARKINSONS_DISEASE
KEGG_PROTEIN_EXPORT
KEGG_RIBOSOME
PLXNA1
B
KEGG_GRAFT_VERSUS_HOST_DISEASE
KEGG_HUNTINGTONS_DISEASE
KEGG_OLFACTORY_TRANSDUCTION
KEGG_OXIDATIVE_PHOSPHORYLATION
KEGG_PARKINSONS_DISEASE
KEGG_RIBOSOME
PLXNA2
C
KEGG_NEUROACTIVE_LIGAND_RECEPTOR_INTERACTION
KEGG_OLFACTORY_TRANSDUCTION
KEGG_PARKINSONS_DISEASE
KEGG_RIBOSOME
PLXNA3
D
KEGG_CITRATE_CYCLE_TCA_CYCLE
KEGG_HOMOLOGOUS_RECOMBINATION
KEGG_MISMATCH_REPAIR
KEGG_OLFACTORY_TRANSDUCTION
KEGG_PROTEIN_EXPORT
KEGG_TERPENOID_BACKBONE_BIOSYNTHESIS
PLXNA4
E
KEGG_GRAFT_VERSUS_HOST_DISEASE
KEGG_OLFACTORY_TRANSDUCTION
KEGG_SYSTEMIC_LUPUS_ERYTHEMATOSUS
PLXNB1
F
KEGG_FRUCTOSE_AND_MANNOSE_METABOLISM
KEGG_GRAFT_VERSUS_HOST_DISEASE
KEGG_OLFACTORY_TRANSDUCTION
KEGG_PRIMARY_IMMUNODEFICIENCY
KEGG_SPHINGOLIPID_METABOLISM
KEGG_VALINE_LEUCINE_AND_ISOLEUCINE_DEGRADATION
PLXNB2
G
KEGG_DNA_REPLICATION
KEGG_NEUROACTIVE_LIGAND_RECEPTOR_INTERACTION
KEGG_OLFACTORY_TRANSDUCTION
KEGG_OXIDATIVE_PHOSPHORYLATION
KEGG_RIBOSOME
KEGG_RNA_DEGRADATION
PLXNB3
H
KEGG_GLYCOSYLPHOSPHATIDYLINOSITOL_GPI_ANCHOR_BIOSYNTHE
KEGG_HOMOLOGOUS_RECOMBINATION
KEGG_MISMATCH_REPAIR
KEGG_OLFACTORY_TRANSDUCTION
KEGG_PROTEIN_EXPORT
KEGG_RNA_POLYMERASE
PLXNC1
I
KEGG_CELL_ADHESION_MOLECULES_CAMS
KEGG_ECM_RECEPTOR_INTERACTION
KEGG_FOCAL_ADHESION
KEGG_NEUROACTIVE_LIGAND_RECEPTOR_INTERACTION
KEGG_OLFACTORY_TRANSDUCTION
KEGG_RIBOSOME
PLXND1
Running Enrichment Score
Ranked List Metric
Rank in Ordered Dataset

Figure 3. Diseases, functional roles, and pathways in COAD were enriched with Plexin members using GSEA. Plexin members: A: PLXNA1; B: PLXNA2; C: PLXNA3; D: PLXNA4; E: PLXNB1; F: PLXNB2; G: PLXNB3; H: PLXNC1; I: PLXND1.

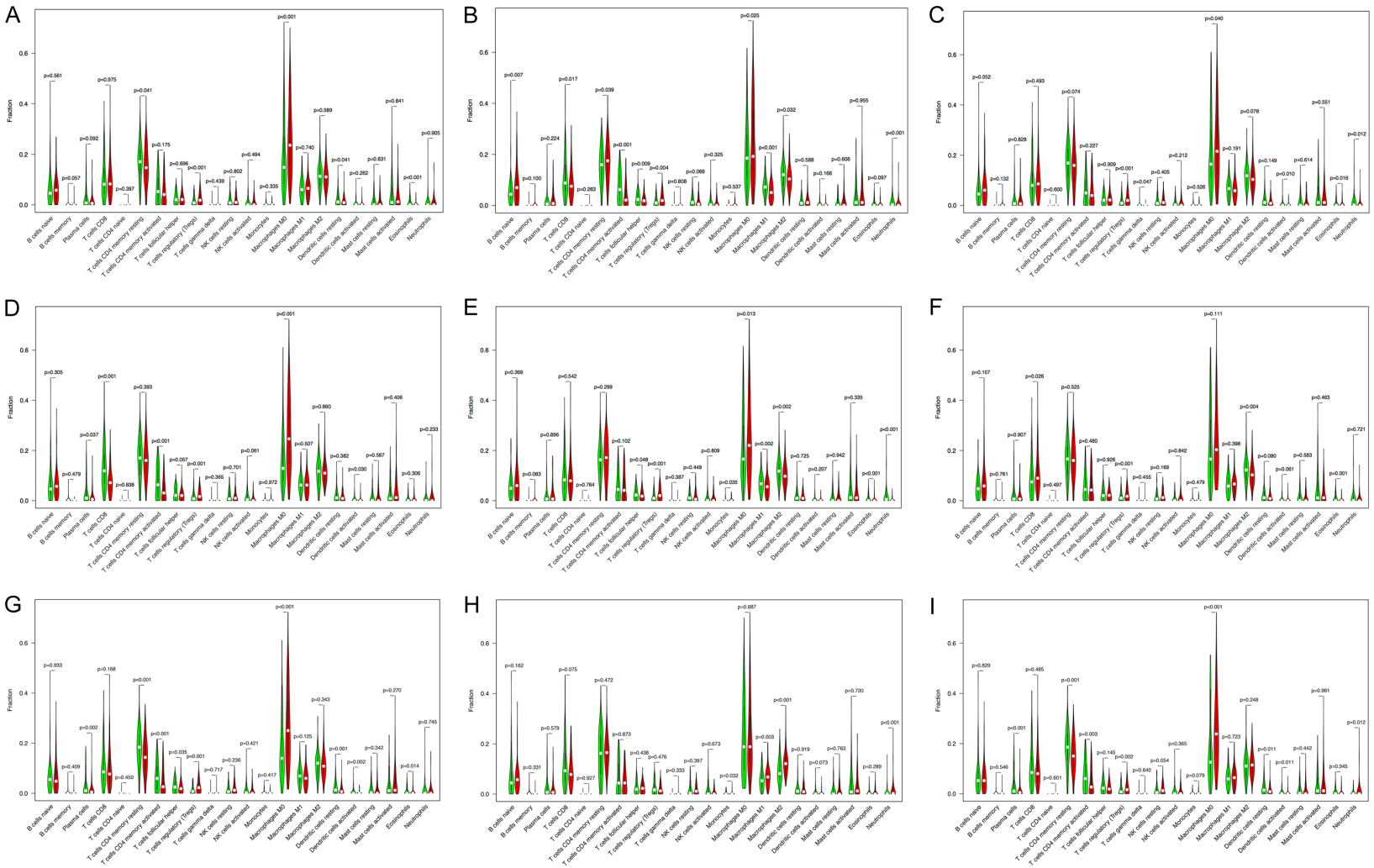

Figure 4. Correlation analysis of Plexins expression with tumor-infiltrating immune cells (TIICs) proportion in COAD. The violin plots display the proportions of 22 TIICs relative to the median Plexins expression in COAD samples. Plexin members: (A) PLXNA1; (B) PLXNA2; (C) PLXNA3; (D) PLXNA4; (E) PLXNB1; (F) PLXNB2; (G) PLXNB3; (H) PLXNC1; (I) PLXND1.

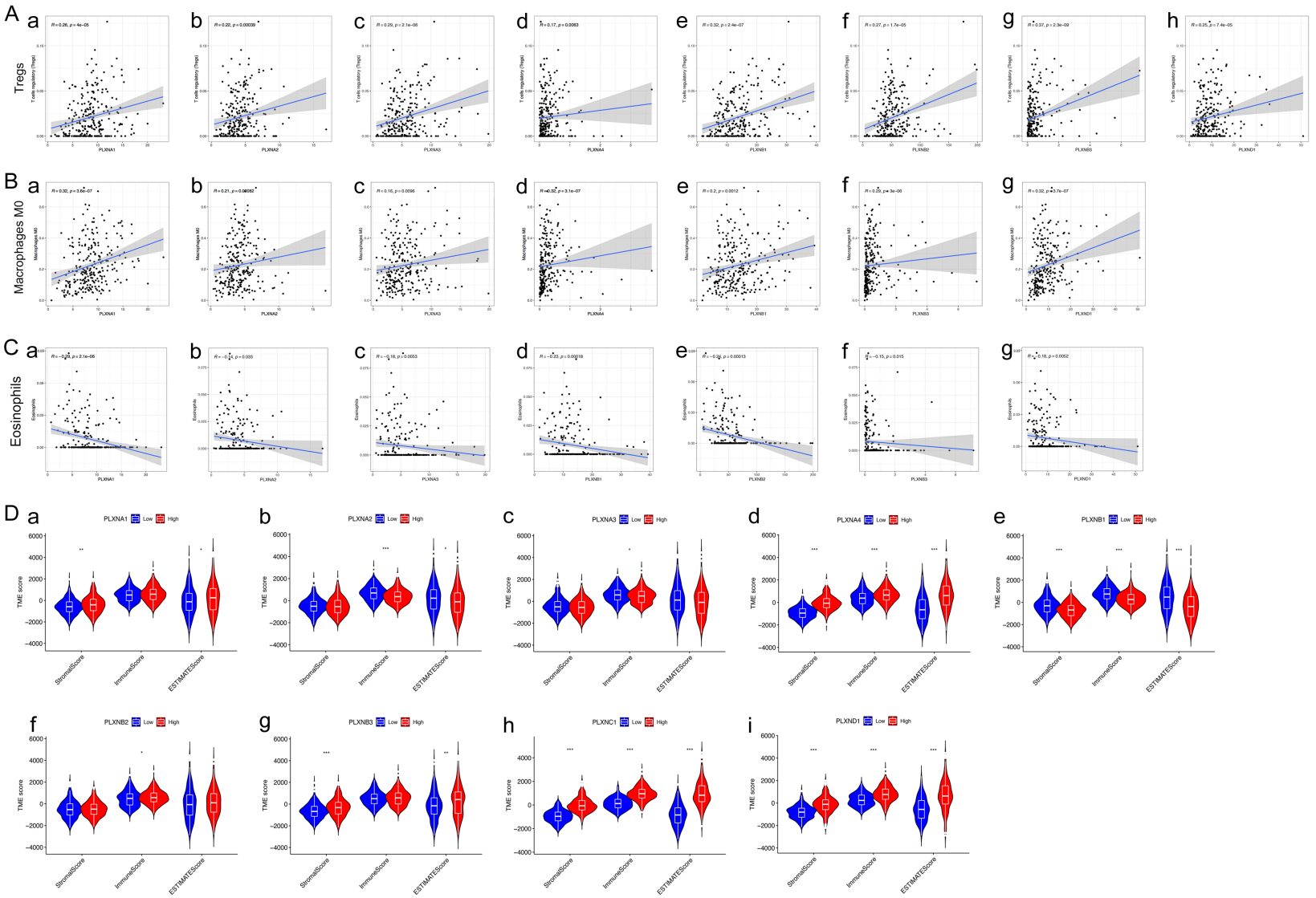

Figure 5. Correlations of Plexin members expression in COAD with T cell regulatory, macrophages M0, and eosinophils proportion. A: Scatter plot displays the correlation of the proportions of T cell regulatory with the expression of Plexin members in COAD. a: PLXNA1; b: PLXNA2; c: PLXNA3; d: PLXNA4; e: PLXNB1; f: PLXNB2; g: PLXNB3; h: PLXND1. B: Scatter plot indicates the correlation of the proportions of Macrophages M0 with the expression of Plexin members in COAD. a: PLXNA1; b: PLXNA2; c: PLXNA3; d: PLXNA4; e: PLXNB1; f: PLXNB3; g: PLXND1. C: Scatter plot reveals the correlation of the proportions of Eosinophils with the expression of Plexin members in COAD. a: PLXNA1; b: PLXNA2; c: PLXNA3; d: PLXNB1; e: PLXNB2; f: PLXNB3; g: PLXND1. D: Correlation of the stromal, immune, and ESTIMATE scores with the expression of Plexin members using the ESTIMATE algorithm. a: PLXNA1; b: PLXNA2; c: PLXNA3; d: PLXNA4; e: PLXNB1; f: PLXNB2; g: PLXNB3; h: PLXNC1; i: PLXND1.

Plexins (excluding PLXNB2 and PLXNC1), the infiltration levels of Macrophages M0 were also enhanced (**Figure 5B**). Except for PLXNA4 and PLXNC1, highly expressed Plexins were negatively correlated with the level of eosinophil infiltration (**Figure 5C**, Supplementary Figure 3). The difference and correlation analysis showed multiple TIICs associated with the expression of Plexin members (Supplementary Table 2). In addition, ESTIMATE analysis confirmed that the high PLXNA4/PLXNC1/PLXND1 expression group had a higher ImmuneScore, StromalScore, and ESTIMATEScore than the low PLXNA4/PLXNC1/PLXND1 expression group. Also, we found that the low PLXNB1 expression group showed higher ImmuneScores, StromalScores, and ESTIMATEScore than the high PLXNB1 expression group (**Figure 5D**). These analyses indicated that a complex immune network existed in COAD and operated in a tightly regulated manner.

Prognostic value of Plexin members in COAD

To investigate the prognostic value of Plexins in TCGA-COAD data. For Plexin molecules, aberrant expression levels of PLXNA3 (P=0.043), PLXNB3 (P=0.002), and PLXND1 (P=0.045) were significantly correlated with worse overall survival of COAD patients (**Figure 6A**). Then, the predictive capabilities of PLXND1 and clinical features (Age, Stage, T, N. M) were demonstrated and connected with poor survival in COAD patients using the univariate Cox regression analysis (Supplementary Table 3). The independent prognostic roles of PLXND1 were evaluated by multivariate Cox regression analysis and displayed on forest plots (**Figure 6B**). The expression level of PLXND1 and two clinical parameters (T stage and Age) were independent prognostic factors in COAD patients (Supplementary Table 4). A predictive nomogram was performed to estimate the 1-, 3-, and 5-year survival rates of patients with COAD based on age, gender, grade, T, N, stage, and PLXND1 expression (**Figure 6C**). The 1-, 3-, and 5-year calibration curves were near the diagonal reference line, indicating good predictive performance (**Figure 6C**). In addition, we predicted the sensitivities to common anticancer drugs, chemotherapeutics, and targeted agents in high- and low-risk groups of COAD patients. The IC_{50} values of Bortezomib, Cyclopamine, Dasatinib, Embelin, Lapatinib, Paclitaxel, Pazopanib, Rapamycin, Ruxolitinib, Saracatinib, and Sunitinib in the high-risk group were lower than those in the low-risk group, indicating that these drugs are more sensitive to the high-risk patients (Supplementary Figure 4). In contrast, the low-risk group was more sensitive to Erlotinib, Pyrimethamine, Salubrinal, Sorafenib, and Vinorelbine (Supplementary Figure 4). The above data revealed that the expression levels of PLXND1 may serve as a potential indicator of prognosis in COAD.

PLXND1 regulatory network, pathways, and mechanisms in COAD

Based on the above analysis, PLXND1 among Plexins was compactly interrelated with the expression profile, immune cell infiltration, and prognosis of COAD samples, indicating that PLXND1 played an essential role in COAD patients. Thus, based on the expression of PLXND1 in COAD, 50 crucial differentially expressed genes were screened. The network plot showed 12 molecules closely correlated to PLXND1 and 38 related molecules (**Figure 7A**). We examined the expression of 12 molecules related to PLXND1 expression based on the TCGA-COAD dataset; the results showed that PDGFB, Notch3, NID2, MMP14, COL18A1, and PDGFRB were up-regulated in COAD samples compared with normal samples. ITGB2, HSPG2, and VWF were downregulated in COAD samples compared to normal samples (Supplementary Figure 5A). GO and KEGG analyses were performed for differentially expressed genes according to the expression level of PLXND1 in COAD. The GO analysis exhibited that the expression of PLXND1 was related to “translation”, “protein binding”, “poly(A) RNA binding”, “membrane”, “extracellular exosome”, “cytoplasm”, “cytosol”, and cell adhesion. The detailed genes for GO enrichment analysis were plotted in **Figure 7B**. KEGG results revealed that the expression level of PLXND1 was related to “ribosome”, “phagosome”, “pathway in cancer”, “Parkinson’s disease”, “metabolic pathways”, “focal adhesion”, “Huntington’s disease”, “EMC-receptor interaction”, and “Alzheimer’s disease”. Similarly, the detailed genes for KEGG-enriched pathways were mapped in **Figure 7C**. Thus, the regulatory molecules, pathways, and networks of PLXND1 exhibited a common and vital role for PLXND1 in COAD. In addition, the GEPIA and ENCORI

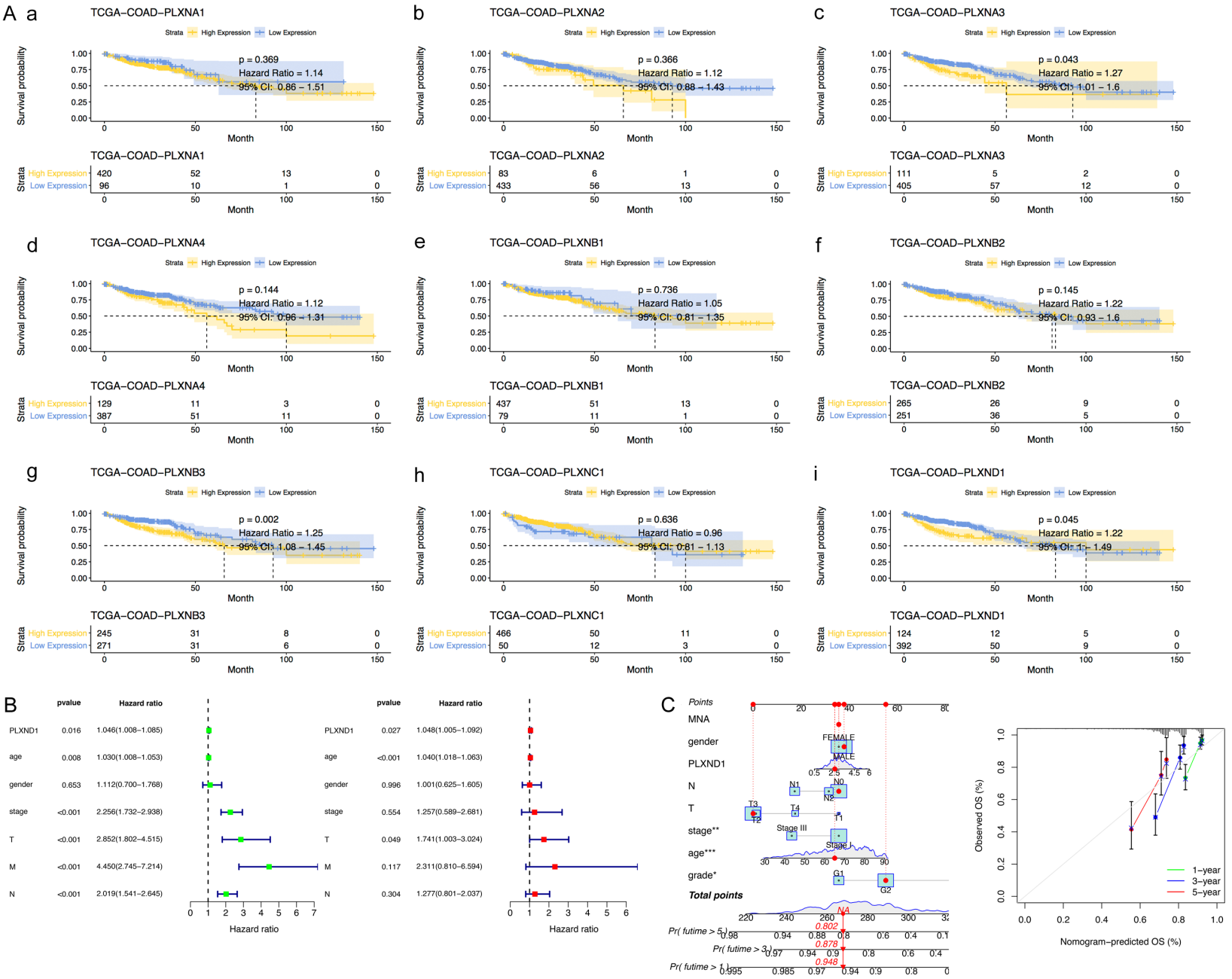
A a
TCGA–COAD–PLXNA1
p = 0.369
Hazard Ratio = 1.14
95% CI: 0.86 – 1.51
b
TCGA–COAD–PLXNA2
p = 0.366
Hazard Ratio = 1.12
95% CI: 0.88 – 1.43
c
TCGA–COAD–PLXNA3
p = 0.043
Hazard Ratio = 1.27
95% CI: 1.01 – 1.6
d
TCGA–COAD–PLXNA4
p = 0.144
Hazard Ratio = 1.12
95% CI: 0.96 – 1.31
e
TCGA–COAD–PLXNB1
p = 0.736
Hazard Ratio = 1.05
95% CI: 0.81 – 1.35
f
TCGA–COAD–PLXNB2
p = 0.145
Hazard Ratio = 1.22
95% CI: 0.93 – 1.6
g
TCGA–COAD–PLXNB3
p = 0.002
Hazard Ratio = 1.25
95% CI: 1.08 – 1.45
h
TCGA–COAD–PLXNC1
p = 0.636
Hazard Ratio = 0.96
95% CI: 0.81 – 1.13
i
TCGA–COAD–PLXND1
p = 0.045
Hazard Ratio = 1.22
95% CI: 1 – 1.49
Strata
High Expression
Low Expression
Survival probability
Month
B
pvalue
Hazard ratio
PLXND1 0.016 1.046(1.008–1.085)
age 0.008 1.030(1.008–1.053)
gender 0.653 1.112(0.700–1.768)
stage <0.001 2.256(1.732–2.938)
T <0.001 2.852(1.802–4.515)
M <0.001 4.450(2.745–7.214)
N <0.001 2.019(1.541–2.645)
PLXND1 0.027 1.048(1.005–1.092)
age <0.001 1.040(1.018–1.063)
gender 0.996 1.001(0.625–1.605)
stage 0.554 1.257(0.589–2.681)
T 0.049 1.741(1.003–3.024)
M 0.117 2.311(0.810–6.594)
N 0.304 1.277(0.801–2.037)
Hazard ratio
C
Points
MNA
gender
PLXND1
N
T
stage**
age***
grade*
Total points
FEMALE
MALE
N1
N0
N2
T3
T4
T2
T1
Stage III
Stage I
G1
G2
Pr(futime > 5)
Pr(futime > 3)
Pr(futime > 1)
0.802
0.878
0.948
Observed OS (%)
Nomogram–predicted OS (%)
1–year
3–year
5–year

Figure 6. Prognostic value of Plexin members in COAD patients. A: Kaplan-Meier survival rates identified the relationship between high and low expression of Plexin members and prognosis in COAD patients. Plexin members: a: PLXNA1; b: PLXNA2; c: PLXNA3; d: PLXNA4; e: PLXNB1; f: PLXNB2; g: PLXNB3; h: PLXNC1; i: PLXND1. B: Forest plot exhibited univariate and multivariate Cox analysis results for PLXND1. C: Nomograms were constructed and validated for 1-, 3-, or 5-year survival in COAD patients. The calibration curve shows the changes in nomograms for predicting overall survival and actual survival.

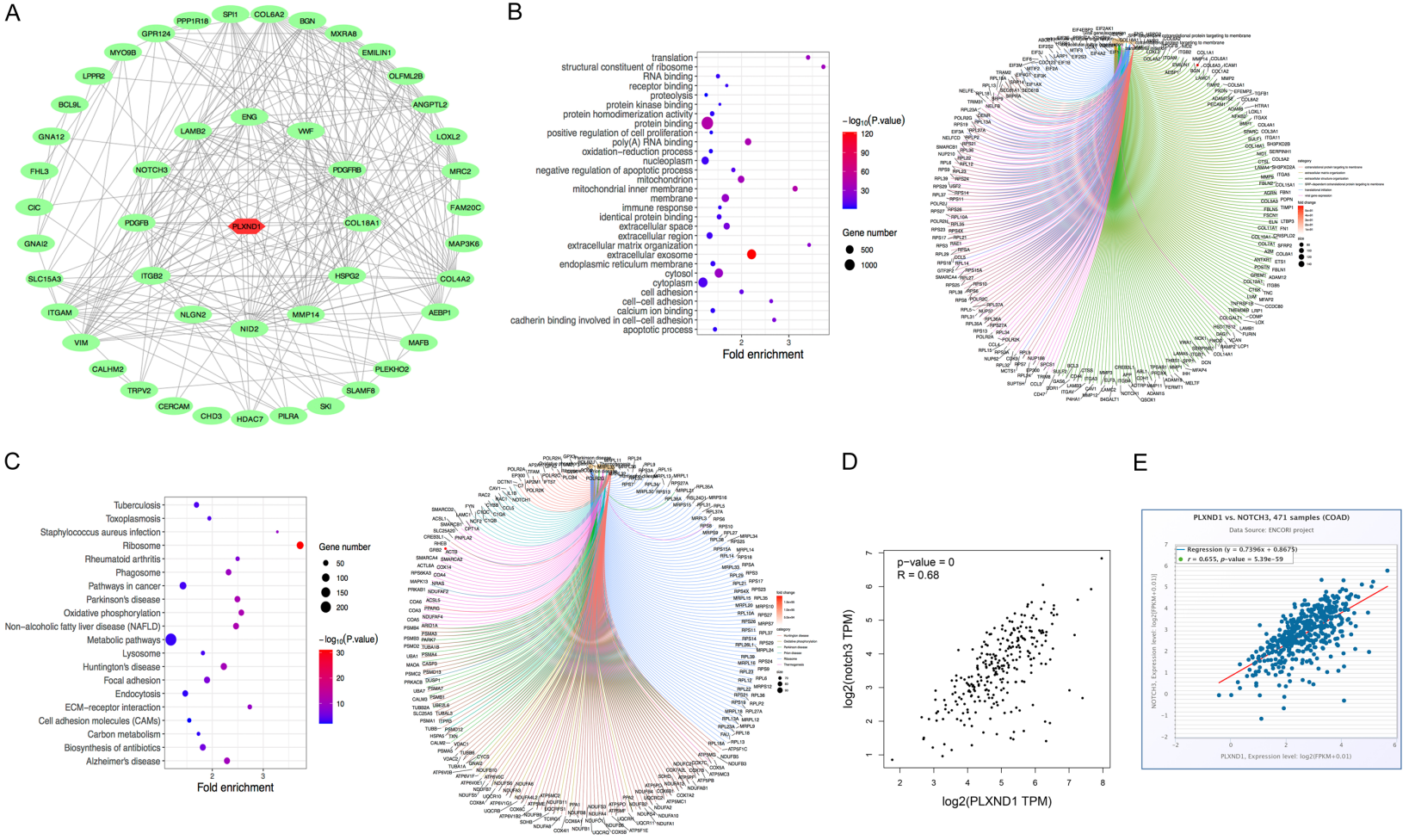

Figure 7. Regulatory network and underlying mechanisms by which PLXND1 affected COAD carcinogenesis. A: Regulatory network of Plexin members and 50 differentially expressed molecules. B: Bubble and circle plots of enriched GO annotations for 50 differentially expressed molecules in COAD. C: Bubble and circle plots of enriched KEGG pathways for 50 differentially expressed molecules in COAD. D: The GEPIA database displays a significant positive correlation between PLXND1 and Notch3 in COAD. E: ENCORI database manifests a significant positive correlation between PLXND1 and Notch3 in COAD.

databases revealed a significant positive correlation between PLXND1 and Notch3 expression levels. Combined with the TCGA data, we analyzed that PLXND1 potentially binds to Notch3 and affects COAD progression, which raised interest for further experimental validation (**Figure 7D**, **7E**).

PLXND1 promotes COAD cell migration, invasion, and EMT by modulating Notch3

Thus, we conducted a series of functional experiments to verify the functional role of PLXND1 in COAD. qRT-PCR assays indicated that the expression of PLXND1 was observably enhanced in 35 COAD tissues in comparison with paired normal tissues (**Figure 8A**). The HPA database revealed that the expression of PLXND1 was upregulated in COAD tissues compared with those in normal colon tissues (**Figure 8B**). Survival analysis revealed that COAD patients with high expression of PLXND1 had shorter survival times compared to the patients with low expression of PLXND1 (**Figure 8C**). The expression of PLXND1 was markedly increased in lymph node-positive COAD patients compared with lymph node-negative COAD patients (**Table 1**), suggesting that PLXND1 may be involved in the metastasis and progression of COAD. IHC assays demonstrated that PLXND1 exhibited higher expression in COAD tissues compared with the normal adjacent tissues (**Figure 8D**). Then, we constructed the HCT8 stable cell line overexpressing PLXND1. The siRNAs targeting PLXND1 were constructed in HCT116 cells, and overexpression and knockdown efficiencies were verified by qRT-PCR, respectively (**Figure 8E**, **8F**). The invasive activity of HCT8 cells was prominently increased after overexpression of PLXND1 by the transwell assays, while knockdown of PLXND1 revealed the opposite results (**Figure 8G**, **8H**). The wound healing assays exhibited that the PLXND1 overexpression group observably enhanced the migration capacity of HCT8 cells compared with the OE-NC group, while the knockdown of PLXND1 restrained the migration activity of HCT116 cells (**Figure 8I**, **8J**). IF assays manifested that E-cadherin expression was down-regulated and Vimentin expression was upregulated after HCT8 cells overexpressed PLXND1. After the knockdown of PLXND1 in HCT116 cells, E-cadherin expression was upregulated, and Vimentin expression was down-regulated (x200 times; **Figure 8K**, **8L**).

Further, IF assays displayed that overexpression of PLXND1 enhanced Notch3 expression levels, while silencing of PLXND1 suppressed the Notch3 expression levels (x200 times; **Figure 9A**, **9B**). WB assays also confirmed that HCT8 cells transfected with overexpression of PLXND1 enhanced Vimentin and Notch3 expression levels while decreasing E-cadherin expression levels. Knockdown of PLXND1 showed the opposite trend (**Figure 9C**, Supplementary Figure 5B). IP and Coomassie brilliant blue staining validated the pull-down of the Notch3 molecule by PLXND1 antibodies (**Figure 9D**). Co-IP and WB experiments confirmed the binding relationship between PLXND1 and Notch3 in COAD (**Figure 9E**). Subsequently, the roles of PLXND1 for tumor growth and metastasis *in vivo* were investigated. The results of the xenograft assay demonstrated that the mice with the overexpression of PLXND1 reduced tumor volume and weight compared to control groups (**Figure 9F-H**). The nude metastasis mouse model indicated that the lung metastatic nodules were observably increased after the overexpression of PLXND1 (**Figure 9I**, **9J**). These data revealed that PLXND1 positively affected tumor growth *in vivo*. Thus, these findings indicated that PLXND1 can affect and promote COAD cell migration, invasion, and EMT ability by regulating Notch3 signaling.

Discussion

The roles of semaphorins and their receptors, Plexins and neuropilins (NRPs), have been increasingly realized and explored in various cancers [17]. Like NRPs, Plexins are also type 1 transmembrane receptors and are segregated into four Type-A plexins, three Type-B plexins, and a single C and D plexin [18]. Studies have shown that Plexins are also dysregulated in different cancer types, and the roles of Plexins in tumor growth, drug resistance, and metastasis have gradually been recognized and investigated [19, 20]. The expression of PLXND1 was increased and promoted prostate cancer progression [6]. PLXNB1 was minimally expressed in both tumor metastasis and immune cell infiltration in breast cancer [7]. Our data were based on multiple databases to determine the expression profile, enrichment analysis,

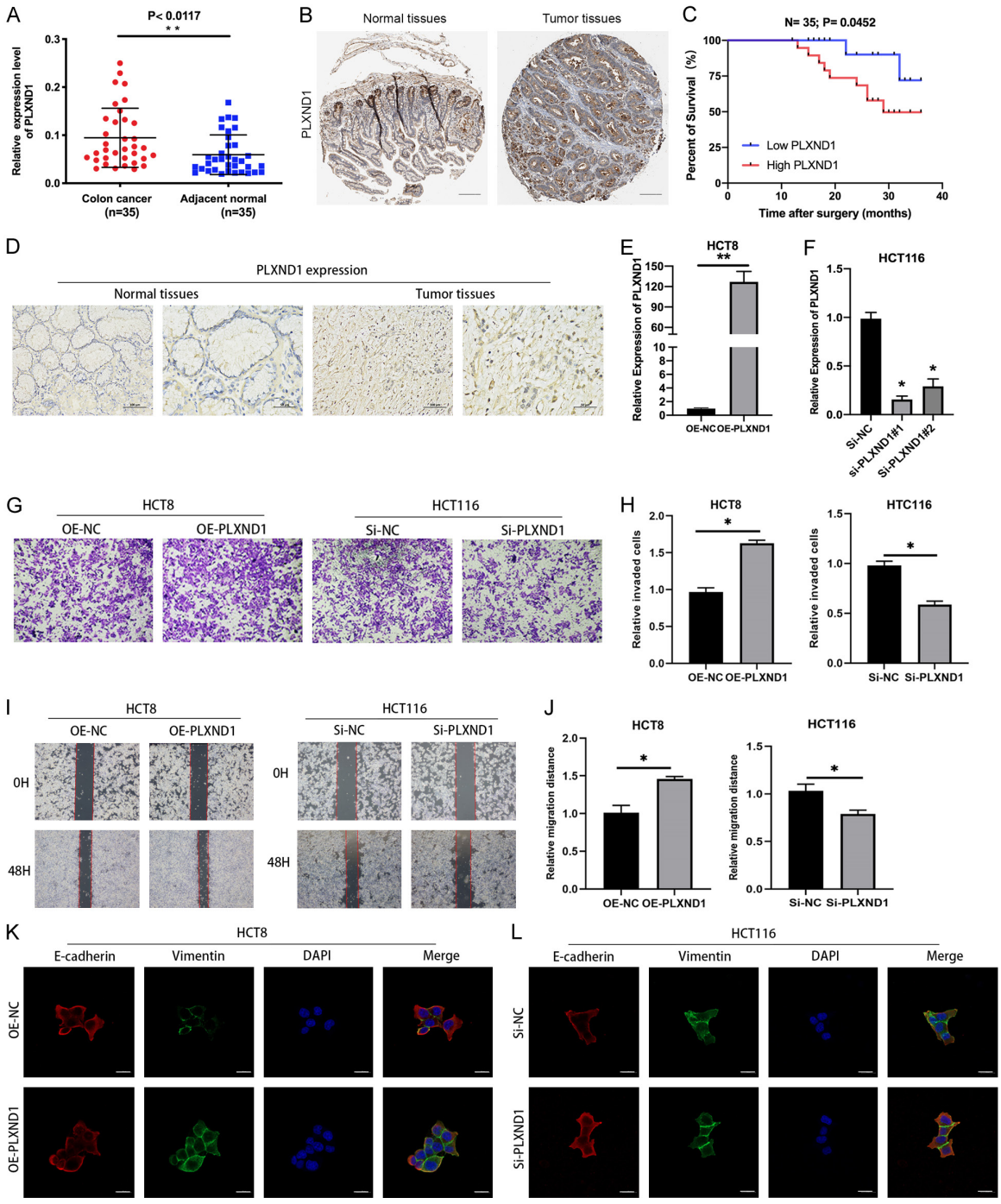

Figure 8. PLXND1 promoted the migration, invasion, and EMT of COAD cells. A: The expression of PLXND1 in 35 paired COAD tissues and normal adjacent tissues was examined by qRT-PCR assays. B: Protein expression of PLXND1 in COAD tissues and normal tissues was detected by HPA data. C: The correlation of PLXND1 expression levels with the prognosis of COAD patients was analyzed using the Kaplan-Meier plotter. D: The expression of PLXND1 in representative COAD tissues and normal tissues was validated by IHC staining. E: The expression of PLXND1 in COAD cells stably transfected with LV5 lentiviral-PLXND1 was tested by qRT-PCR. F: The expression of PLXND1 in COAD cells treated with siRNA was validated by qRT-PCR. G, H: Transwell assays verified the invasion ability of cells after the overexpression of PLXND1. I, J: Wound healing assays demonstrated the migration ability of cells after the overexpression of PLXND1. K, L: The fluorescence intensities of E-cadherin and Vimentin after PLXND1 overexpression or knockdown were confirmed by IF assays. *P<0.05; **P<0.01.

Table 1. Relationship between the expression of PLXND1 and clinicopathologic variables in 35 patients with COAD

Patient Characteristics	Total	PLXND1 expression		*P* Value
		Low	High	
Age				0.990
≤65	21	11	10	
>65	14	8	6	
Gender				0.723
Male	25	13	12	
Female	10	6	4	
Tumor size (cm)				0.181
≤5	16	10	6	
>5	19	7	12	
TNM stage				0.092
I/II	18	13	5	
III/IV	17	7	10	
Distant metastasis				0.990
No	33	18	15	
Yes	2	1	1	
Lymph node status				0.041*
Negative	16	12	4	
Positive	19	7	12	

*P value <0.05.

immune infiltration, and prognostic value of the Plexins family in COAD. An in-depth study of the family screened PLXND1 as a key molecule, differentially highly expressed in COAD. PLXND1 levels were correlated with lymph node metastasis, immune cell infiltration, and a worse prognosis in COAD. Thus, we further performed molecular and signaling pathway analysis as well as detailed functional experimental validation of the PLXND1.

This study demonstrated that Plexins have different expression levels in 23 cancer types in TCGA pan-cancer data. Meanwhile, most Plexin members were positively correlated in COAD samples, suggesting that Plexins may have cooperative roles in carcinogenesis and progression of COAD. Most Plexins were differentially expressed in COAD samples and normal samples and showed similar differences in COAD cells, indicating that Plexins exhibit a degree of heterogeneity in COAD tissues and cells. The expression levels of PLXNA3 and PLXNB3 rose gradually with the increase in the clinical T, N, and M stages, suggesting that COAD patients with high expression of PLXNB3 and PLXNA3 had later T stage, N stage, and M stage. Strikingly, many Plexins (PLXNA3, PLXNA4, PLXNB3, and PLXND1) were expressed more dramatically in the high node (N) stage than in the N0 stage, indicating that the expression of Plexins was involved in lymph node metastasis. Some Plexin members synergize and interrelate with multiple factors regulating COAD tumorigenesis and progression. Therefore, we conducted the GSEA analyses on COAD samples and manifested that the functions of highly expressed Plexins were primarily related to axon guidance, focal adhesion, ECM receptor interaction, T/B cell receptors, pathways in cancer, semaphoring plexin signaling, and semaphoring receptor activity. The functions of low-expressed Plexins were chiefly associated with Alzheimer's disease, Huntington's disease, and others.

Since many Plexins are enriched for T/B cell receptors, we examined the relationship between Plexins and immune cell infiltration in COAD. Previous studies have reported that Plexins are novel immunomodulatory molecules with distinct roles at different stages of the immune responses [21, 22]. The role of plexins depended on the environment and cellular differentiation, many of which had complex effects on the immune system; several plexins were essential for maintaining immune homeostasis [23, 24]. Thus, this study analyzed the differences and correlations between Plexins and immune cell infiltration. We discovered that natural killer cells, macrophages M2, T cell CD4 memory resting, and macrophages M0 accounted for most TIICs in COAD by studying the expression of Plexins. High expression levels of PLXNA2, PLXNA3, PLXNB1, PLXNB3, and PLXND1 were associated with aggressive subtypes that promoted immune infiltration. In contrast, the expression levels of PLXNB2 and PLXNC1 were not closely related to the subtype of immune-infiltrating subtypes. Then, the data demonstrated that, in addition to PLXNB2, PLXNA4, and PLXNC1, high expression of Plexins not only markedly enhanced the infiltration of Macrophages M0 and Tregs, but also the expression of Plexins positively correlated with Tregs and Macrophages M0 infiltration. However, the high expression of Plexins showed the opposite trend in eosinophils. Many articles have reported that Treg cells are vital in maintaining immune homeostasis by suppressing T

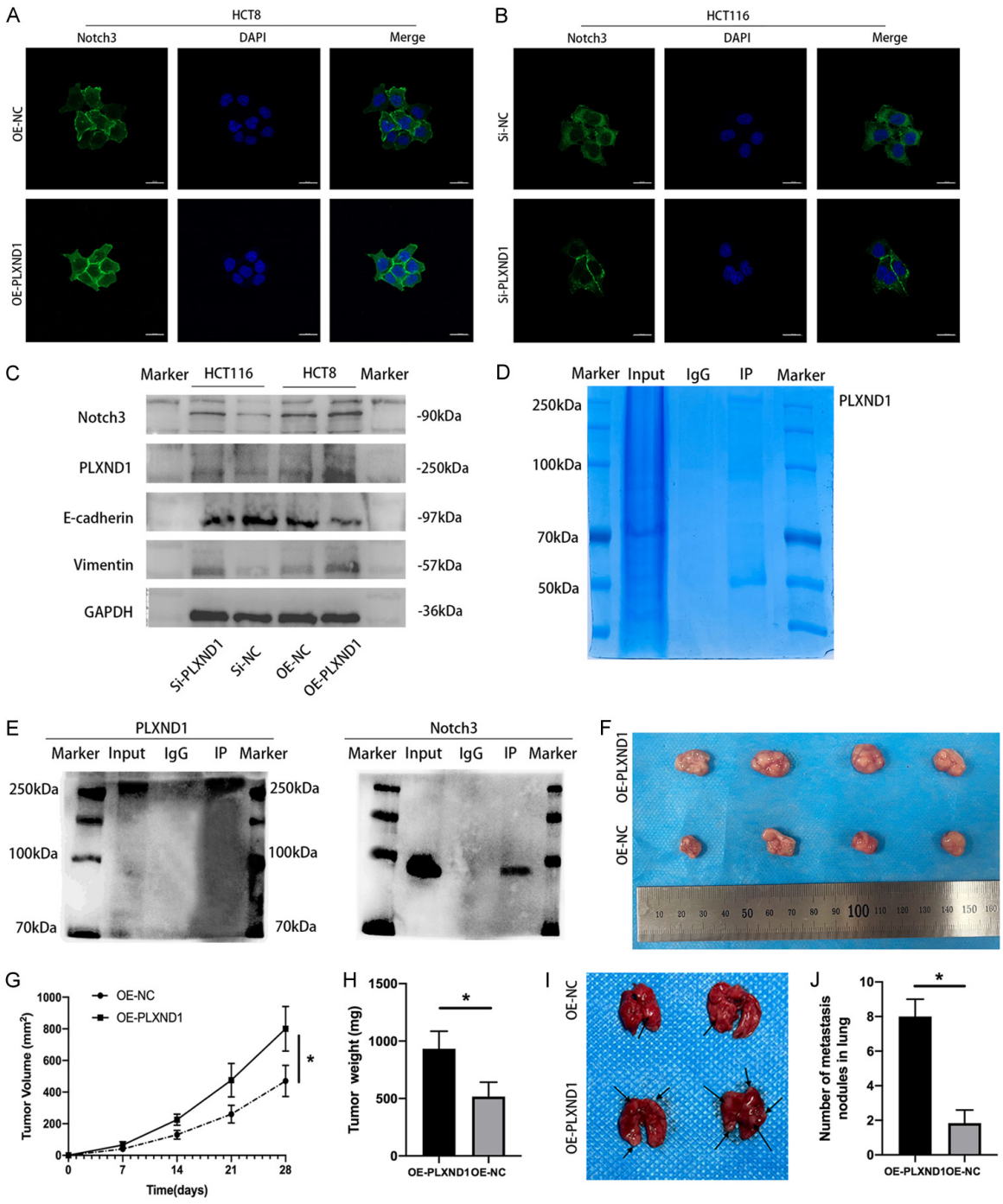

Figure 9. PLXND1 promoted the metastasis and EMT ability of COAD by modulating Notch3. A, B: The fluorescence intensity of Notch3 after PLXND1 overexpression or knockdown was verified by IF assays. C: The expression of PLXND1, Notch3, E-cadherin, and Vimentin after PLXND1 overexpression or knockdown was determined by WB assays. D: IP experiments were performed to extract the proteins from COAD cells using the PLXND1 antibody. The proteins were separated by SDS-PAGE followed by Coomassie brilliant blue staining. E: CO-IP experiments confirmed the interaction between PLXND1 and Notch3 in COAD cells. F: Image of subcutaneous tumor tissues in the PLXND1-overexpressing group and control group. G, H: Volume and weight of subcutaneous tumor tissues in each group. I, J: Image of lung metastatic nodules in the PLXND1 overexpression and the OE-NC groups is indicated by arrows. *P<0.05; **P<0.01.

cell responses and functions through various direct or indirect mechanisms. The number and proportion of Treg cells in peripheral blood, tumor tissue, and lymph nodes of tumor

patients are increased, with the highest number of Treg cells in tumor tissues [25, 26]. The expression of the Plexin family was positively associated with Treg cells, suggesting that Plexins can be involved in the role of Treg cells in maintaining immune homeostasis in COAD patients. Farha et al. reported that M0 macrophage enrichment has a worse prognosis and a lower predicted immune checkpoint blockade (ICB) response in renal clear cell carcinoma [27]. The expression of most Plexins was positively associated with M0, M1, or M2 macrophages, indicating that Plexins may be involved in regulating the role of M0, M1, or M2 macrophages in COAD. In addition, Wang et al. showed that the negative correlation between eosinophil count and overall cancer risk suggests that eosinophils may contribute to tumor immune surveillance [28]. Our results revealed that highly expressed Plexins (Except for PLXNA4 and PLXNC1) were negatively correlated with eosinophil levels in COAD. The above data indicated that the expression levels of most Plexins in COAD were associated with the infiltration of Tregs, Macrophages M0, and Eosinophils, indicating that most Plexins can directly or indirectly regulate the COAD immune response network.

Some articles have reported that Plexin molecules have been involved in the prognosis of tumor patients [14, 24]. For example, Li noted that the PLXND1 molecule may be a target and valuable prognostic biomarker for liver cancer [29]. PLXNC1 can serve as an independent biomarker and facilitates gastric cancer progression by transcriptional activation of IL6ST [30]. The higher mRNA levels of PLXNA2 had a dramatically higher survival rate in patients with glioma [31]. Our study examined the high expression of PLXNA3, PLXNB3, and PLXND1, which was positively correlated with poorer survival in COAD patients. Afterward, univariate Cox analyses indicated that PLXND1 was notably associated with poorer survival outcomes. Multivariate Cox analyses displayed that the PLXND1, T stage, and age were independent prognostic factors in COAD patients. A nomogram with clinical data and PLXND1 expression was constructed, showing high predictive performance. We not only found that the levels of PLXNA3, PLXNB3, and PLXND1 were relevant to the worse prognosis of COAD patients, but PLXND1 also served as a prognostic indicator, suggesting that the expression levels of some Plexin members may guide the prognosis of COAD patients. Furthermore, chemotherapy and targeted therapy are current strategies to treat COAD; it is critical to understand the effectiveness and sensitivity of these drugs to different risk groups. The pRRophetic package was used to analyze drugs with high-risk sensitivity to PLXND1 (Bortezomib, Cyclopamine, Dasatinib, Embelin, Lapatinib, Paclitaxel, Pazopanib, Rapamycin, Ruxolitinib, Saracatinib, and Sunitinib), and low-risk sensitivity to PLXND1 (Erlotinib, Pyrimethamine, Salubrinal, Sorafenib, and Vinorelbine). PLXND1 expression may be a biomarker of prognosis and a therapeutic target for COAD patients.

Combined with the above findings, PLXND1 was correlated with clinical data, immune infiltration, and poor prognosis of COAD patients. We further examined the mRNA and protein levels of PLXND1 in the COAD samples exceeded those in normal samples, suggesting that PLXND1 had a specific value in the progression of COAD. Our data showed that the expression of PLXND1 was markedly increased in COAD tissues and lymph node-positive COAD patients, suggesting that PLXND1 may be involved in the metastasis and progression of COAD. Also, high expression of PLXND1 went with shorter survival times compared to the patients with low expression of PLXND1, which was consistent with the predictions of bioinformatics. Then, we screened and examined 12 genes that were closely correlated to PLXND1 and differentially expressed in COAD. PLXND1 differential molecules were associated, including Notch3, which might be involved in regulating the PLXND1. PLXND1 was engaged in “translation”, “protein binding”, “poly(A) RNA binding”, “extracellular exosome”, “cytoplasm”, “cytosol”, and cell adhesion. The KEGG enrichment results of Plexins were similar to the GSEA results, which may function through cell membranes, exosomes, and adhesion. Next, a series of experiments verified that PLXND1 could promote COAD cell invasion, migration, and EMT *in vitro* and *in vivo*. By bioinformatic analysis, we noted the molecule and found that Notch3 signaling promotes colorectal cancer growth by enhancing immunosuppressive cell infiltration in the microenvironment [32]. Kuan Shen et al. reported the use of branched-chain amino acid metabolism and Notch3 expression to predict

and target colorectal cancer progression [33]. Notch3 is also closely related to tumor progression and immune infiltration. We further validated that PLXND1 can bind to Notch3 in COAD by IP and CO-IP experiments, and WB and IF results indicated that PLXND1 promotes COAD invasion and metastasis by affecting and regulating Notch3 expression. PLXND1 may play a role in promoting tumor invasion, metastasis and EMT through Notch3 in COAD. Based on these findings, the PLXND1 and Notch3 molecules may have mutual synergistic effects in cancer progression and tumor-associated immune infiltration. Admittedly, our study has some limitations. Our data is primarily based on bioinformatics analysis and has certain background heterogeneity. Each Plexin member's specific mechanisms in COAD may differ, and further experimental studies are needed.

Conclusion

These findings demonstrate that some Plexin members play vital roles in metastasis, immune infiltration, and the prognostic value of COAD patients. PLXND1 was screened as an independent prognostic biomarker and promoted the invasion, metastasis, and EMT of COAD cells by binding Notch3. These data provide new perspectives to investigate the role of Plexin molecules in COAD progression and to exert targeted therapeutic effects.

Acknowledgements

The authors expressed their sincere thanks to all the databases used in this study. The research team thanked Zeen Wang for his contribution to data analysis. This research was funded by the National Natural Science Foundation of China (No. 82103257).

Informed consent was obtained from all subjects involved in the study. Written informed consent has been obtained from the patient(s) to publish this paper.

Disclosure of conflict of interest

None.

Address correspondence to: Drs. Xinglong Dai and Ziwei Wang, Gastrointestinal Surgical Unit, The First Affiliated Hospital of Chongqing Medical University, No. 1 Youyi Road, Yuan Jiagang, Yuzhong District, Chongqing 400042, PR China. E-mail: daixinglong@hospital.cqmu.edu.cn (XLD); dxl_123abc@163.com (ZWW)

References

[1] Bray F, Laversanne M, Sung H, Ferlay J, Siegel RL, Soerjomataram I and Jemal A. Global cancer statistics 2022: GLOBOCAN estimates of incidence and mortality worldwide for 36 cancers in 185 countries. CA Cancer J Clin 2024; 74: 229-263.

[2] Wadhwa V, Patel N, Grover D, Ali FS and Thosani N. Interventional gastroenterology in oncology. CA Cancer J Clin 2023; 73: 286-319.

[3] Toledano S and Neufeld G. Plexins as regulators of cancer cell proliferation, migration, and invasivity. Cancers (Basel) 2023; 15: 4046.

[4] Fard D, Giraudo E and Tamagnone L. Mind the (guidance) signals! Translational relevance of semaphorins, plexins, and neuropilins in pancreatic cancer. Trends Mol Med 2023; 29: 817-829.

[5] Limoni G and Niquille M. Semaphorins and Plexins in central nervous system patterning: the key to it all? Curr Opin Neurobiol 2021; 66: 224-232.

[6] Chen B, Xu P, Yang JC, Nip C, Wang L, Shen Y, Ning S, Shang Y, Corey E, Gao AC, Gestwicki JE, Wei Q, Liu L and Liu C. Plexin D1 emerges as a novel target in the development of neural lineage plasticity in treatment-resistant prostate cancer. Oncogene 2024; 43: 2325-2337.

[7] Franzolin G, Brundu S, Cojocaru CF, Curatolo A, Ponzo M, Mastrantonio R, Mihara E, Kumanogoh A, Suga H, Takagi J, Tamagnone L and Giraudo E. PlexinB1 Inactivation Reprograms Immune Cells in the Tumor Microenvironment, Inhibiting Breast Cancer Growth and Metastatic Dissemination. Cancer Immunol Res 2024; 12: 1286-1301.

[8] Bernard A, Eggstein C, Tang L, Keller M, Körner A, Mirakaj V and Rosenberger P. Plexin C1 influences immune response to intracellular LPS and survival in murine sepsis. J Biomed Sci 2024; 31: 82.

[9] Hu J, Zhang J, Han B, Qu Y, Zhang Q, Yu Z, Zhang L, Han J, Liu H, Gao L, Feng T, Dou B, Chen W and Sun F. PLXNA1 confers enzalutamide resistance in prostate cancer via AKT signaling pathway. Neoplasia 2024; 57: 101047.

[10] Toledano S, Sabag AD, Ilan N, Liburkin-Dan T, Kessler O and Neufeld G. Plexin-A2 enables the proliferation and the development of tumors from glioblastoma derived cells. Cell Death Dis 2023; 14: 41.

[11] Zuo Q, Yang Y, Lyu Y, Yang C, Chen C, Salman S, Huang TY, Wicks EE, Jackson W 3rd, Datan E, Qin W and Semenza GL. Plexin-B3 expression

stimulates MET signaling, breast cancer stem cell specification, and lung metastasis. Cell Rep 2023; 42: 112164.
[12] Moreno P, Fexova S, George N, Manning JR, Miao Z, Mohammed S, Muñoz-Pomer A, Fullgrabe A, Bi Y, Bush N, Iqbal H, Kumbham U, Solovyev A, Zhao L, Prakash A, García-Seisdedos D, Kundu DJ, Wang S, Walzer M, Clarke L, Osumi-Sutherland D, Tello-Ruiz MK, Kumari S, Ware D, Eliasova J, Arends MJ, Nawijn MC, Meyer K, Burdett T, Marioni J, Teichmann S, Vizcaíno JA, Brazma A and Papatheodorou I. Expression Atlas update: gene and protein expression in multiple species. Nucleic Acids Res 2022; 50: D129-D140.
[13] Newman AM, Steen CB, Liu CL, Gentles AJ, Chaudhuri AA, Scherer F, Khodadoust MS, Esfahani MS, Luca BA, Steiner D, Diehn M and Alizadeh AA. Determining cell type abundance and expression from bulk tissues with digital cytometry. Nat Biotechnol 2019; 37: 773-782.
[14] Zhao X, Yu X, Li W, Chen Z, Niu T, Weng X, Wang L and Liu X. CDK6 as a biomarker for immunotherapy, drug sensitivity, and prognosis in bladder cancer: bioinformatics and immunohistochemical analysis. Int J Med Sci 2024; 21: 2414-2429.
[15] Uhlén M, Fagerberg L, Hallström BM, Lindskog C, Oksvold P, Mardinoglu A, Sivertsson Å, Kampf C, Sjöstedt E, Asplund A, Olsson I, Edlund K, Lundberg E, Navani S, Szigyarto CA, Odeberg J, Djureinovic D, Takanen JO, Hober S, Alm T, Edqvist PH, Berling H, Tegel H, Mulder J, Rockberg J, Nilsson P, Schwenk JM, Hamsten M, von Feilitzen K, Forsberg M, Persson L, Johansson F, Zwahlen M, von Heijne G, Nielsen J and Pontén F. Proteomics. Tissue-based map of the human proteome. Science 2015; 347: 1260419.
[16] Shannon P, Markiel A, Ozier O, Baliga NS, Wang JT, Ramage D, Amin N, Schwikowski B and Ideker T. Cytoscape: a software environment for integrated models of biomolecular interaction networks. Genome Res 2003; 13: 2498-504.
[17] Borrelli C, Roberts M, Eletto D, Hussherr MD, Fazilaty H, Valenta T, Lafzi A, Kretz JA, Guido Vinzoni E, Karakatsani A, Adivarahan S, Mannhart A, Kimura S, Meijs A, Baccouche Mhamedi F, Acar IE, Handler K, Ficht X, Platt RJ, Piscuoglio S and Moor AE. In vivo interaction screening reveals liver-derived constraints to metastasis. Nature 2024; 632: 411-418.
[18] Wagner W, Ochman B and Wagner W. Semaphorin 6 family-an important yet overlooked group of signaling proteins involved in cancerogenesis. Cancers (Basel) 2023; 15: 5536.
[19] Mukhwana N, Garg R, Azad A, Mitchell AR and Williamson M. B-type Plexins Regulate Mitosis via RanGTPase. Mol Cancer Res 2025; 23: 8-19.
[20] Hung YH, Hou YC, Hsu SH, Wang LY, Tsai YL, Shan YS, Su YY, Hung WC and Chen LT. Pancreatic cancer cell-derived semaphorin 3A promotes neuron recruitment to accelerate tumor growth and dissemination. Am J Cancer Res 2023; 13: 3417-3432.
[21] Li CX, Long D and Meng Q. Promising therapeutic targets in kidney renal clear cell carcinoma: PLXNA1 and PLXNB3. Cancer Biother Radiopharm 2024; 39: 276-290.
[22] Chapoval SP, Gao H, Fanaroff R and Keegan AD. Plexin B1 controls Treg numbers, limits allergic airway inflammation, and regulates mucins. Front Immunol 2024; 14: 1297354.
[23] Celus W, Oliveira AI, Rivis S, Van Acker HH, Landeloos E, Serneels J, Cafarello ST, Van Herck Y, Mastrantonio R, Köhler A, Garg AD, Flamand V, Tamagnone L, Marine JC, Di Matteo M, Costa BM, Bechter O and Mazzone M. Plexin-A4 mediates cytotoxic T-cell trafficking and exclusion in cancer. Cancer Immunol Res 2022; 10: 126-141.
[24] Hu B, Yang XB and Sang XT. Molecular subtypes based on immune-related genes predict the prognosis for hepatocellular carcinoma patients. Int Immunopharmacol 2021; 90: 107164.
[25] Kumagai S, Itahashi K and Nishikawa H. Regulatory T cell-mediated immunosuppression orchestrated by cancer: towards an immuno-genomic paradigm for precision medicine. Nat Rev Clin Oncol 2024; 21: 337-353.
[26] Iglesias-Escudero M, Arias-González N and Martínez-Cáceres E. Regulatory cells and the effect of cancer immunotherapy. Mol Cancer 2023; 22: 26.
[27] Farha M, Nallandhighal S, Vince R, Cotta B, Stangl-Kremser J, Triner D, Morgan TM, Palapattu GS, Cieslik M, Vaishampayan U, Udager AM and Salami SS. Analysis of the tumor immune microenvironment (TIME) in clear cell renal cell carcinoma (ccRCC) reveals an M0 macrophage-enriched subtype: an exploration of prognostic and biological characteristics of this immune phenotype. Cancers (Basel) 2023; 15: 5530.
[28] Wang JH, Rabkin CS, Engels EA and Song M. Associations between eosinophils and cancer risk in the UK Biobank. Int J Cancer 2024; 155: 486-492.
[29] Li J, Hu K, He D, Zhou L, Wang Z and Tao Y. Prognostic value of PLXND1 and TGF-β1 coexpression and its correlation with immune infiltrates in hepatocellular carcinoma. Front Oncol 2021; 10: 604131.
[30] Chen J, Liu H, Chen J, Sun B, Wu J and Du C. PLXNC1 enhances carcinogenesis through

transcriptional activation of IL6ST in gastric cancer. Front Oncol 2020; 10: 33.
[31] Valiulyte I, Steponaitis G, Kardonaite D, Tamasauskas A and Kazlauskas A. A SEMA3 signaling pathway-based multi-biomarker for prediction of glioma patient survival. Int J Mol Sci 2020; 21: 7396.
[32] Huang K, Luo W, Fang J, Yu C, Liu G, Yuan X, Liu Y and Wu W. Notch3 signaling promotes colorectal tumor growth by enhancing immunosuppressive cells infiltration in the microenvironment. BMC Cancer 2023; 23: 55.
[33] Shen K, Zhu C, Wu J, Yan J, Li P, Cao S, Zhou X and Yao G. Exploiting branched-chain amino acid metabolism and Notch3 expression to predict and target colorectal cancer progression. Front Immunol 2024; 15: 1430352.

Role of the Plexins and PLXND1 in colon cancer

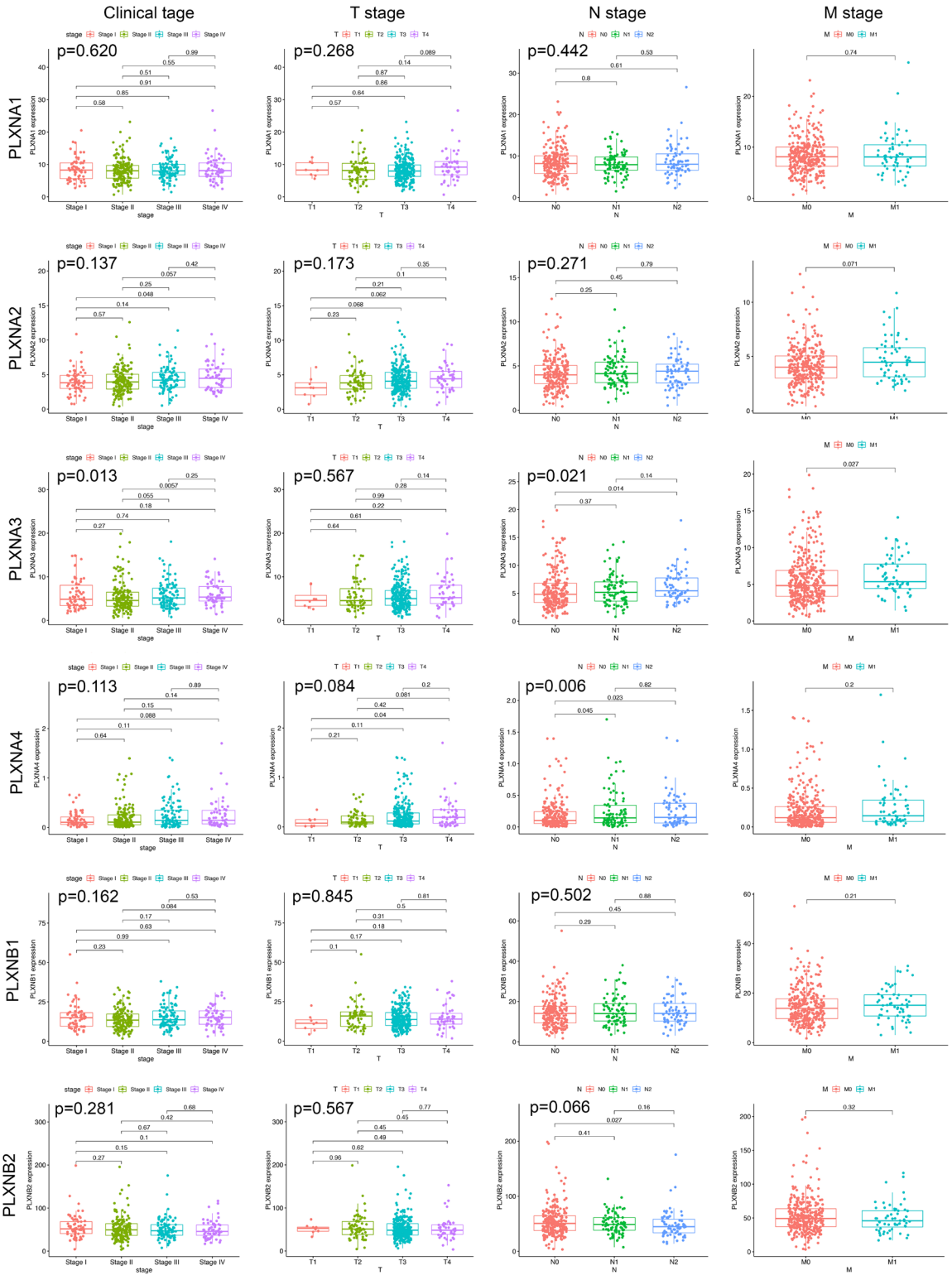

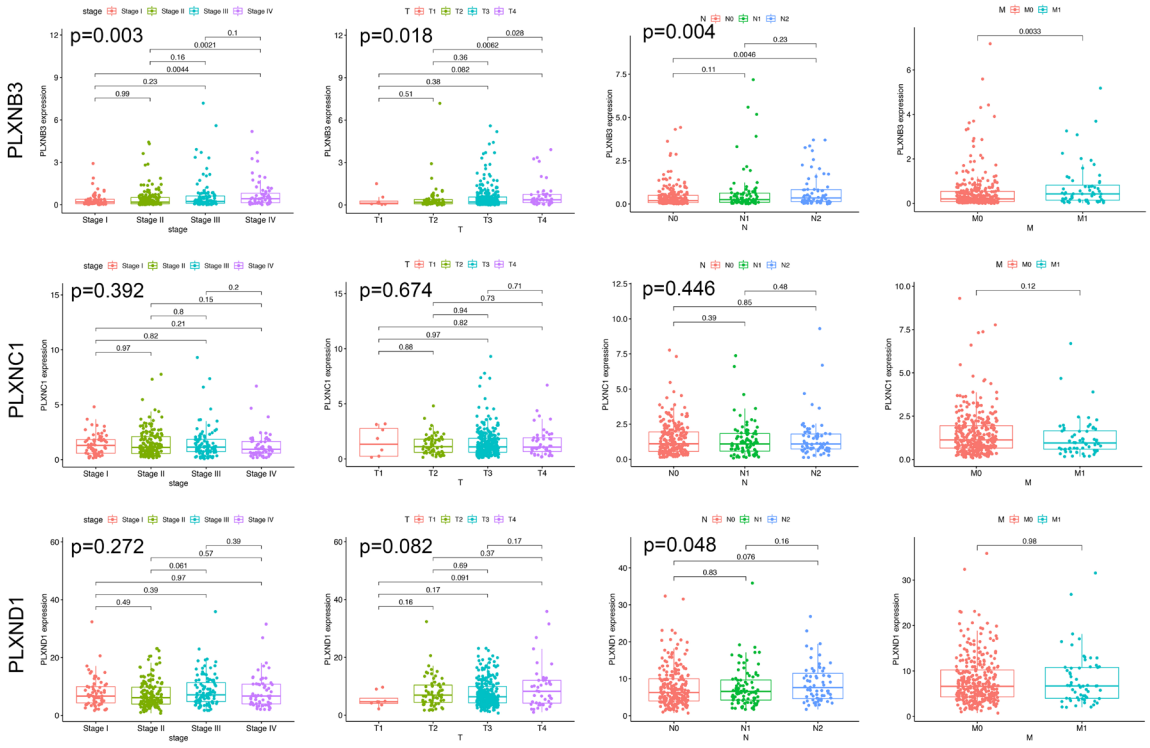

Supplementary Figure 1. Correlation analysis of clinical stage, T stage, N stage, and M stage and the expression of Plexin family members in 452 COAD samples.

A

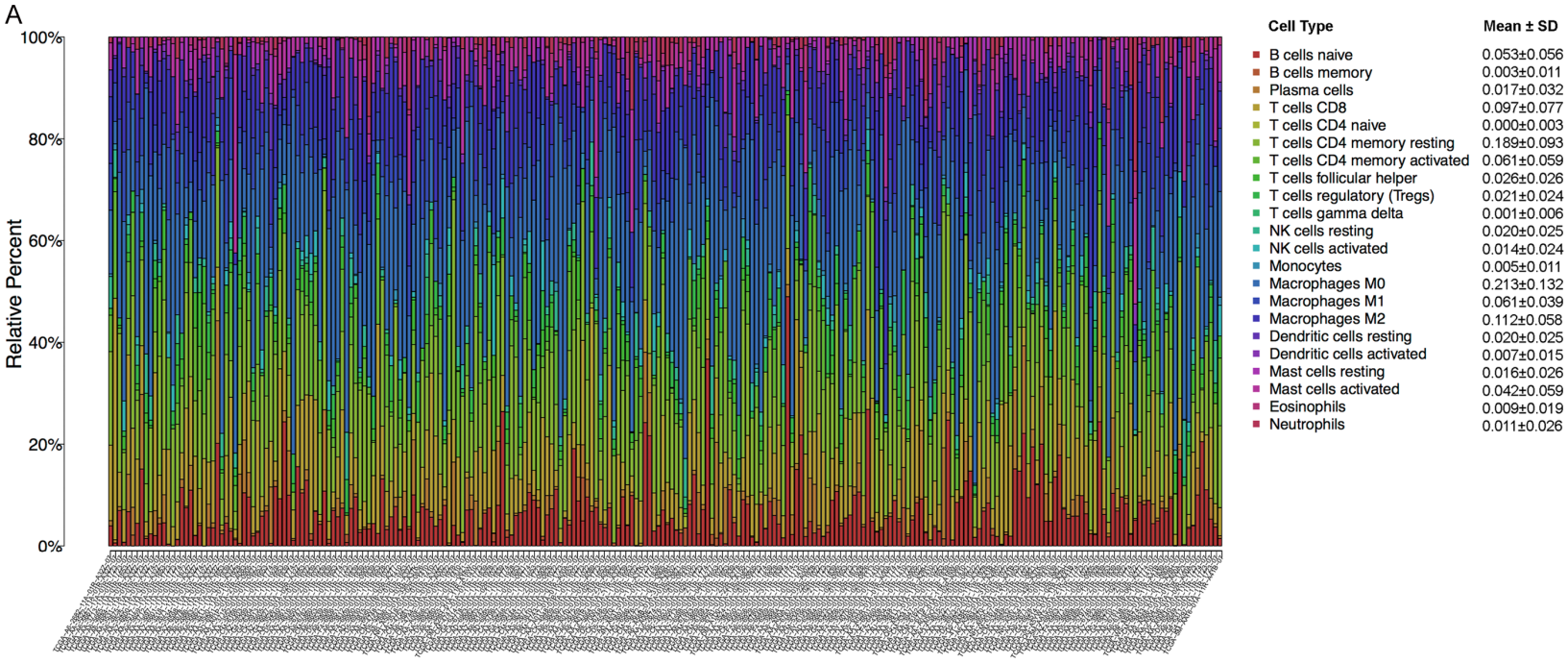
Relative Percent
100%
80%
60%
40%
20%
0%
Cell Type
Mean ± SD
B cells naive 0.053±0.056
B cells memory 0.003±0.011
Plasma cells 0.017±0.032
T cells CD8 0.097±0.077
T cells CD4 naive 0.000±0.003
T cells CD4 memory resting 0.189±0.093
T cells CD4 memory activated 0.061±0.059
T cells follicular helper 0.026±0.026
T cells regulatory (Tregs) 0.021±0.024
T cells gamma delta 0.001±0.006
NK cells resting 0.020±0.025
NK cells activated 0.014±0.024
Monocytes 0.005±0.011
Macrophages M0 0.213±0.132
Macrophages M1 0.061±0.039
Macrophages M2 0.112±0.058
Dendritic cells resting 0.020±0.025
Dendritic cells activated 0.007±0.015
Mast cells resting 0.016±0.026
Mast cells activated 0.042±0.059
Eosinophils 0.009±0.019
Neutrophils 0.011±0.026

B

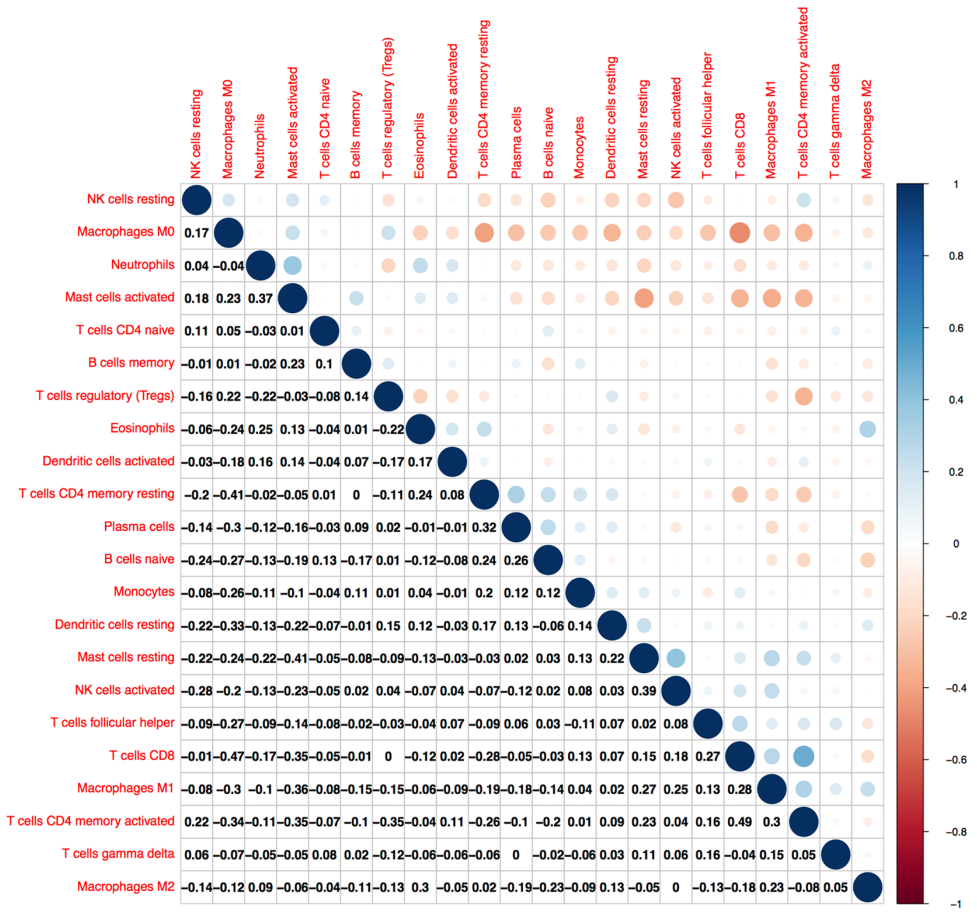

Supplementary Figure 2. A: The proportion of 22 kinds of TIICs in each COAD sample. Each column represents one sample, and each row represents the abundance ratio of immune cells (Mean ± SD) via different colors and heights. B: The correlation of the 22 kinds of TIICs and numeric. Blue is a positive correlation; red is a negative correlation.

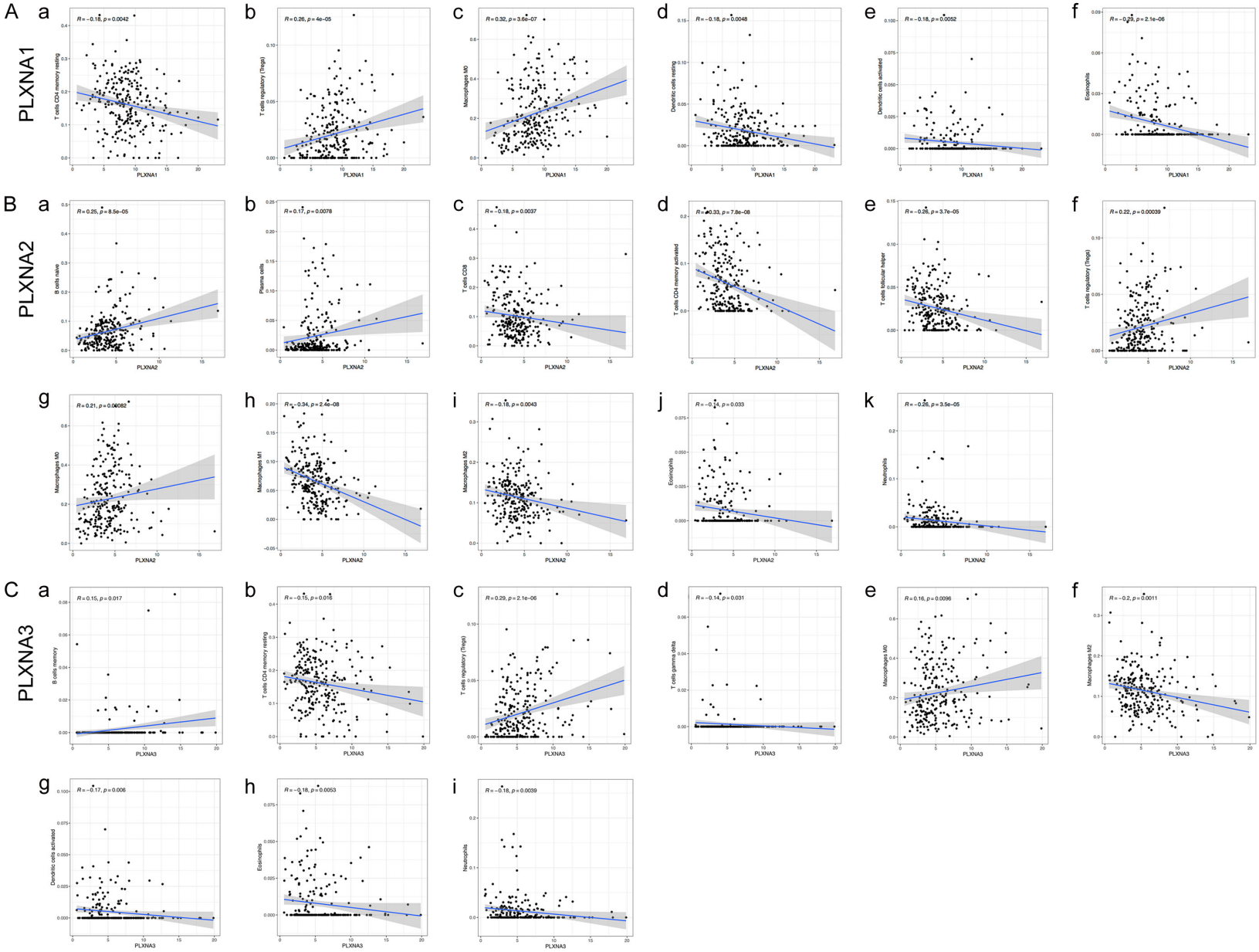
A
PLXNA1
a
R = −0.18, p = 0.0042
T cells CD4 memory resting
PLXNA1
b
R = 0.26, p = 4e−05
T cells regulatory (Tregs)
PLXNA1
c
R = 0.32, p = 3.6e−07
Macrophages M0
PLXNA1
d
R = −0.18, p = 0.0048
Dendritic cells resting
PLXNA1
e
R = −0.18, p = 0.0052
Dendritic cells activated
PLXNA1
f
R = −0.23, p = 2.1e−06
Eosinophils
PLXNA1
B
PLXNA2
a
R = 0.25, p = 8.5e−05
B cells naive
PLXNA2
b
R = 0.17, p = 0.0078
Plasma cells
PLXNA2
c
R = −0.18, p = 0.0037
T cells CD8
PLXNA2
d
R = −0.33, p = 7.8e−08
T cells CD4 memory activated
PLXNA2
e
R = −0.26, p = 3.7e−05
T cells follicular helper
PLXNA2
f
R = 0.22, p = 0.00039
T cells regulatory (Tregs)
PLXNA2
g
R = 0.21, p = 0.00082
Macrophages M0
PLXNA2
h
R = −0.34, p = 2.4e−08
Macrophages M1
PLXNA2
i
R = −0.18, p = 0.0043
Macrophages M2
PLXNA2
j
R = −0.14, p = 0.033
Eosinophils
PLXNA2
k
R = −0.26, p = 3.5e−05
Neutrophils
PLXNA2
C
PLXNA3
a
R = 0.15, p = 0.017
B cells memory
PLXNA3
b
R = −0.15, p = 0.016
T cells CD4 memory resting
PLXNA3
c
R = 0.29, p = 2.1e−06
T cells regulatory (Tregs)
PLXNA3
d
R = −0.14, p = 0.031
T cells gamma delta
PLXNA3
e
R = 0.16, p = 0.0096
Macrophages M0
PLXNA3
f
R = −0.2, p = 0.0011
Macrophages M2
PLXNA3
g
R = −0.17, p = 0.006
Dendritic cells activated
PLXNA3
h
R = −0.18, p = 0.0053
Eosinophils
PLXNA3
i
R = −0.18, p = 0.0039
Neutrophils
PLXNA3

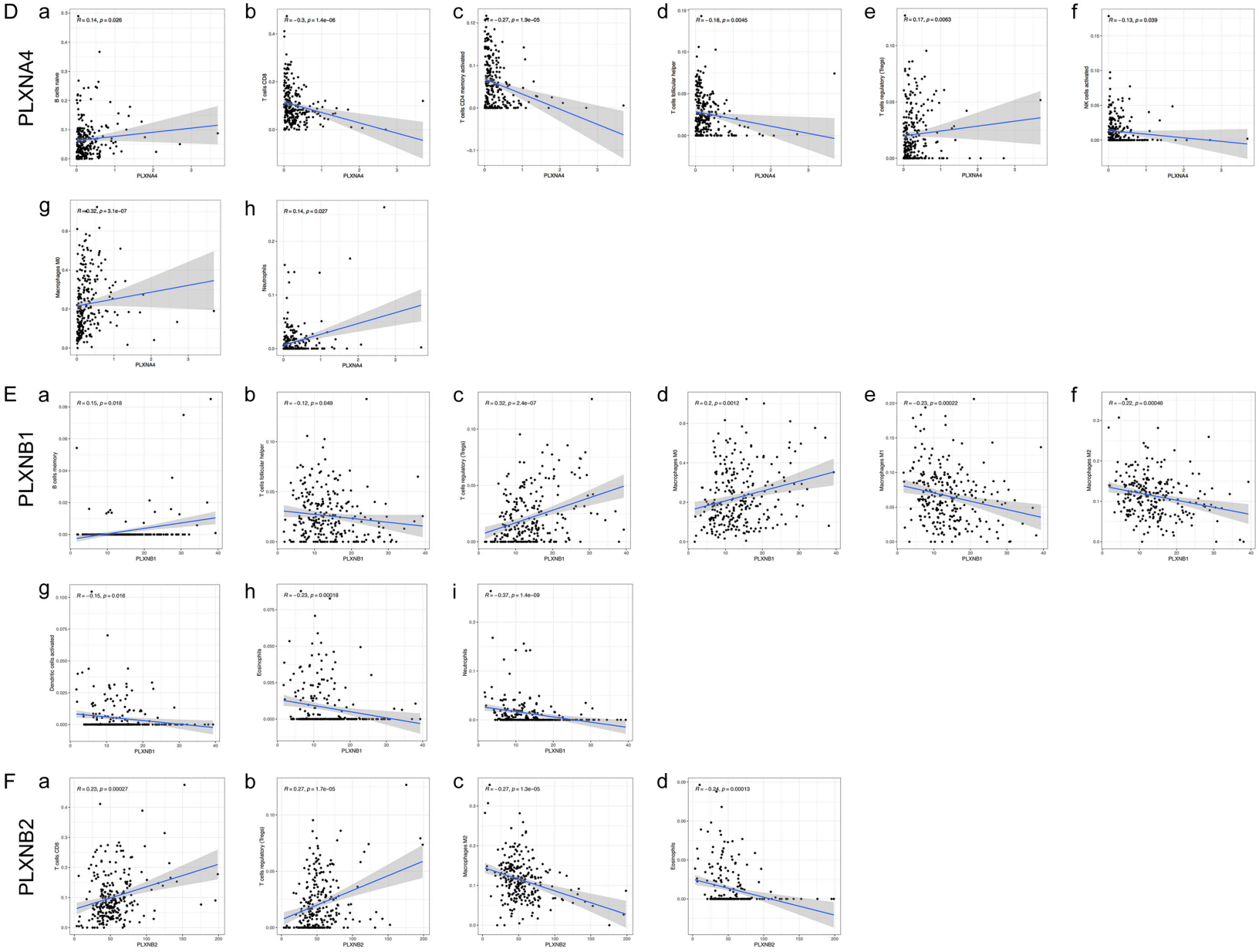
D
PLXNA4
a
R = 0.14, p = 0.026
B cells naive
PLXNA4
b
R = −0.3, p = 1.4e−06
T cells CD8
PLXNA4
c
R = −0.27, p = 1.9e−05
T cells CD4 memory activated
PLXNA4
d
R = −0.18, p = 0.0045
T cells follicular helper
PLXNA4
e
R = 0.17, p = 0.0063
T cells regulatory (Tregs)
PLXNA4
f
R = −0.13, p = 0.039
NK cells activated
PLXNA4
g
R = 0.32, p = 3.1e−07
Macrophages M0
PLXNA4
h
R = 0.14, p = 0.027
Neutrophils
PLXNA4
E
PLXNB1
a
R = 0.15, p = 0.018
B cells memory
PLXNB1
b
R = −0.12, p = 0.049
T cells follicular helper
PLXNB1
c
R = 0.32, p = 2.4e−07
T cells regulatory (Tregs)
PLXNB1
d
R = 0.2, p = 0.0012
Macrophages M0
PLXNB1
e
R = −0.23, p = 0.00022
Macrophages M1
PLXNB1
f
R = −0.22, p = 0.00046
Macrophages M2
PLXNB1
g
R = −0.15, p = 0.016
Dendritic cells activated
PLXNB1
h
R = −0.23, p = 0.00018
Eosinophils
PLXNB1
i
R = −0.37, p = 1.4e−09
Neutrophils
PLXNB1
F
PLXNB2
a
R = 0.23, p = 0.00027
T cells CD8
PLXNB2
b
R = 0.27, p = 1.7e−05
T cells regulatory (Tregs)
PLXNB2
c
R = −0.27, p = 1.3e−05
Macrophages M2
PLXNB2
d
R = −0.34, p = 0.00013
Eosinophils
PLXNB2

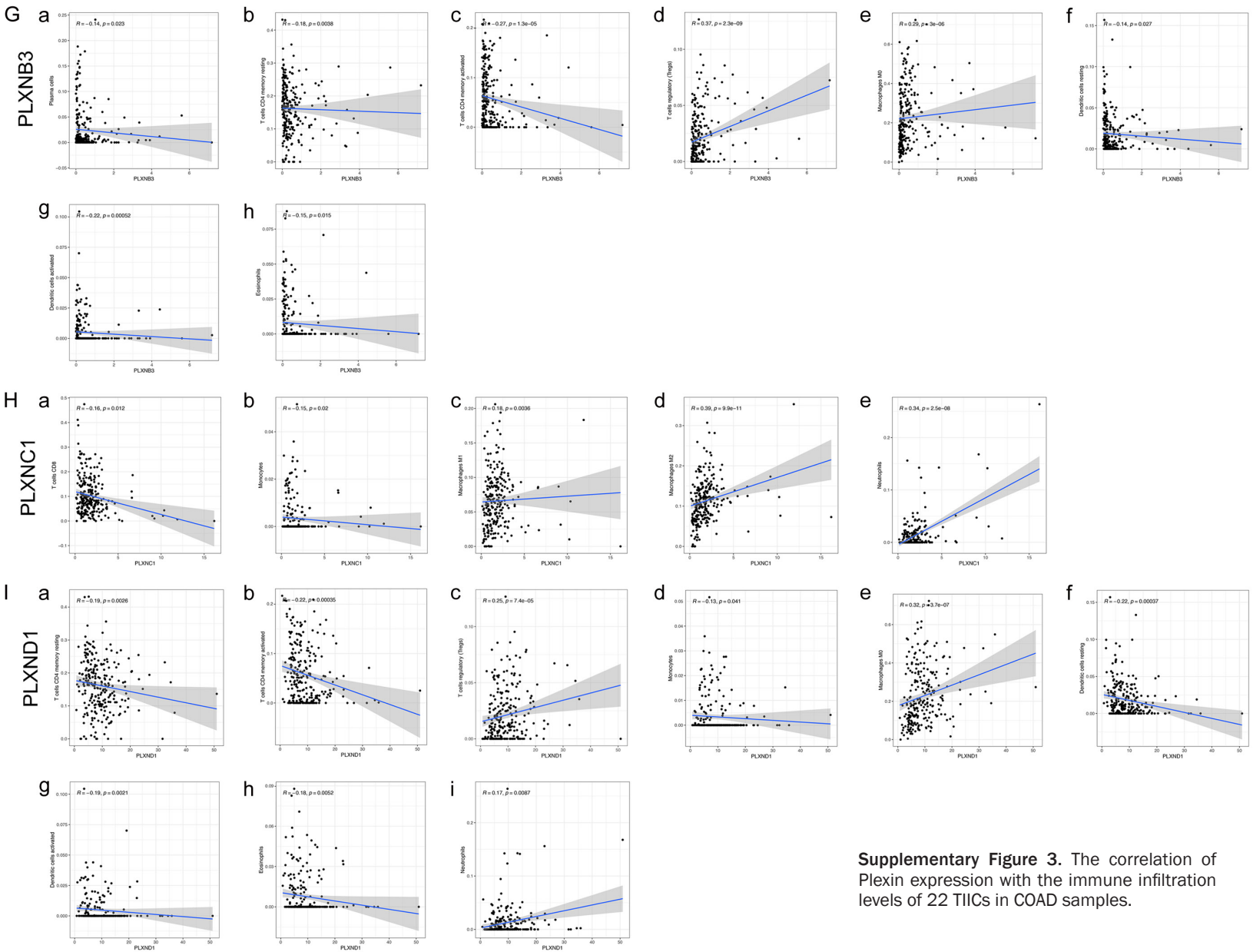

Supplementary Figure 3. The correlation of Plexin expression with the immune infiltration levels of 22 TIICs in COAD samples.

Supplementary Table 1. GSEA analysis for Plexin family members in COAD samples in detail

Supplementary Table 2. Co-screening Plexins-related TIICs in COAD samples by differential and correlation analysis

Gene ID	Plexins-related TIICs
PLXNA1	T cells CD4 memory resting, T cells regulatory (Tregs), Macrophages M0, Dendritic cells resting, Eosinophils
PLXNA2	B cells naïve, T cells CD8, T cells CD4 memory resting, T cells CD4 memory activated, T cells follicular helper, T cells regulatory (Tregs), Macrophages M0, Macrophages M1, Macrophages M2, Neutrophils
PLXNA3	T cells regulatory (Tregs), T cells gamma delta, Macrophages M0, Dendritic cells activated Eosinophils, Neutrophils
PLXNA4	T cells CD8, T cells CD4 memory activated, T cells regulatory (Tregs), Macrophages M0
PLXNB1	T cells follicular helper, T cells regulatory (Tregs), Macrophages M0, Macrophages M1, Macrophages M2, Eosinophils, Neutrophils
PLXNB2	T cells CD8, T cells regulatory (Tregs), Macrophages M2, Eosinophils
PLXNB3	Plasma cells, T cells CD4 memory resting, T cells CD4 memory activated, T cells regulatory (Tregs), Macrophages M0, Dendritic cells resting, Dendritic cells activated, Eosinophils
PLXNC1	Monocytes, Macrophages M1, Macrophages M2, Neutrophils
PLXND1	T cells CD4 memory resting, T cells CD4 memory activated, T cells regulatory (Tregs), Macrophages M0, Dendritic cells resting, Dendritic cells activated, Eosinophils, Neutrophils

Supplementary Table 3. Univariate cox regression analysis of Plexin members and clinical features with overall survival in COAD patients

Parameter	Univariate analysis			
	Hazard Ratio (HR)	HR.95L	HR.95H	*P* value
Age	1.030	1.008	1.053	0.0077*
Gender	1.112	0.700	1.768	0.6533
Stage	2.256	1.732	2.938	1.59E-09*
T	2.852	1.802	4.515	7.77E-06*
M	4.450	2.745	7.214	1.40E-09*
N	2.019	1.541	2.645	3.47E-07*
PLXNA1	1.058	0.992	1.127	0.0868
PLXNA2	1.003	0.884	1.137	0.9664
PLXNA3	1.045	0.975	1.119	0.2113
PLXNA4	2.111	0.895	4.979	0.0878
PLXNB1	0.988	0.954	1.023	0.4930
PLXNB2	1.000	0.990	1.011	0.9417
PLXNB3	1.227	0.994	1.515	0.0575
PLXNC1	1.038	0.858	1.255	0.7036
PLXND1	1.046	1.008	1.085	0.0162*

**P* value <0.05.

Supplementary Table 4. Multivariate analysis of Plexin members and clinical features with overall survival in COAD patients

id	Hazard Ratio (HR)	HR.95L	HR.95H	*P* value	Hazard Ratio (HR)	HR.95L	HR.95H	*P* value	Hazard Ratio (HR)	HR.95L	HR.95H	*P* value
age	1.042	1.019	1.065	0.000*	1.039	1.016	1.063	0.001*	1.040	1.017	1.064	0.001*
gender	1.004	0.627	1.609	0.985	0.977	0.610	1.563	0.922	0.971	0.608	1.553	0.904
stage	1.366	0.636	2.934	0.425	1.326	0.614	2.865	0.473	1.332	0.618	2.870	0.465
T	1.743	1.004	3.025	0.048*	1.778	1.022	3.092	0.042*	1.772	1.016	3.093	0.044*
M	1.796	0.635	5.078	0.270	1.877	0.662	5.318	0.236	1.856	0.656	5.253	0.244
N	1.332	0.838	2.118	0.225	1.351	0.839	2.177	0.216	1.343	0.841	2.145	0.216
PLXNA1	1.061	0.998	1.129	0.058								
PLXNA2					1.010	0.891	1.145	0.875				
PLXNA3									1.048	0.969	1.134	0.237
age	1.041	1.018	1.065	0.001*	1.039	1.016	1.062	0.001*	1.038	1.016	1.061	0.001*
gender	1.013	0.629	1.633	0.957	0.955	0.597	1.529	0.848	0.996	0.621	1.598	0.988
stage	1.333	0.613	2.897	0.468	1.349	0.629	2.891	0.442	1.282	0.596	2.759	0.525
T	1.770	1.014	3.090	0.045*	1.743	1.002	3.031	0.049*	1.789	1.027	3.114	0.040*
M	1.833	0.647	5.193	0.254	1.932	0.688	5.422	0.211	1.976	0.701	5.566	0.198
N	1.327	0.822	2.141	0.247	1.356	0.844	2.178	0.208	1.394	0.864	2.250	0.173
PLXNA4	1.612	0.663	3.920	0.292								
PLXNB1					0.974	0.938	1.011	0.166				
PLXNB2									1.005	0.994	1.016	0.373
age	1.038	1.016	1.062	0.001*	1.039	1.017	1.062	0.001*	1.040	1.018	1.063	0.000*
gender	0.988	0.616	1.583	0.959	0.997	0.620	1.604	0.991	1.001	0.625	1.605	0.996
stage	1.308	0.605	2.825	0.495	1.347	0.623	2.915	0.449	1.257	0.589	2.681	0.554
T	1.808	1.041	3.143	0.036*	1.783	1.025	3.102	0.041*	1.741	1.003	3.024	0.049*
M	1.921	0.678	5.447	0.219	1.887	0.668	5.329	0.231	2.311	0.810	6.594	0.117
N	1.322	0.822	2.127	0.249	1.324	0.822	2.134	0.249	1.277	0.801	2.037	0.304
PLXNB3	1.091	0.840	1.417	0.515								
PLXNC1					1.065	0.880	1.289	0.518				
PLXND1									1.048	1.005	1.092	0.027*

**P* value <0.05.

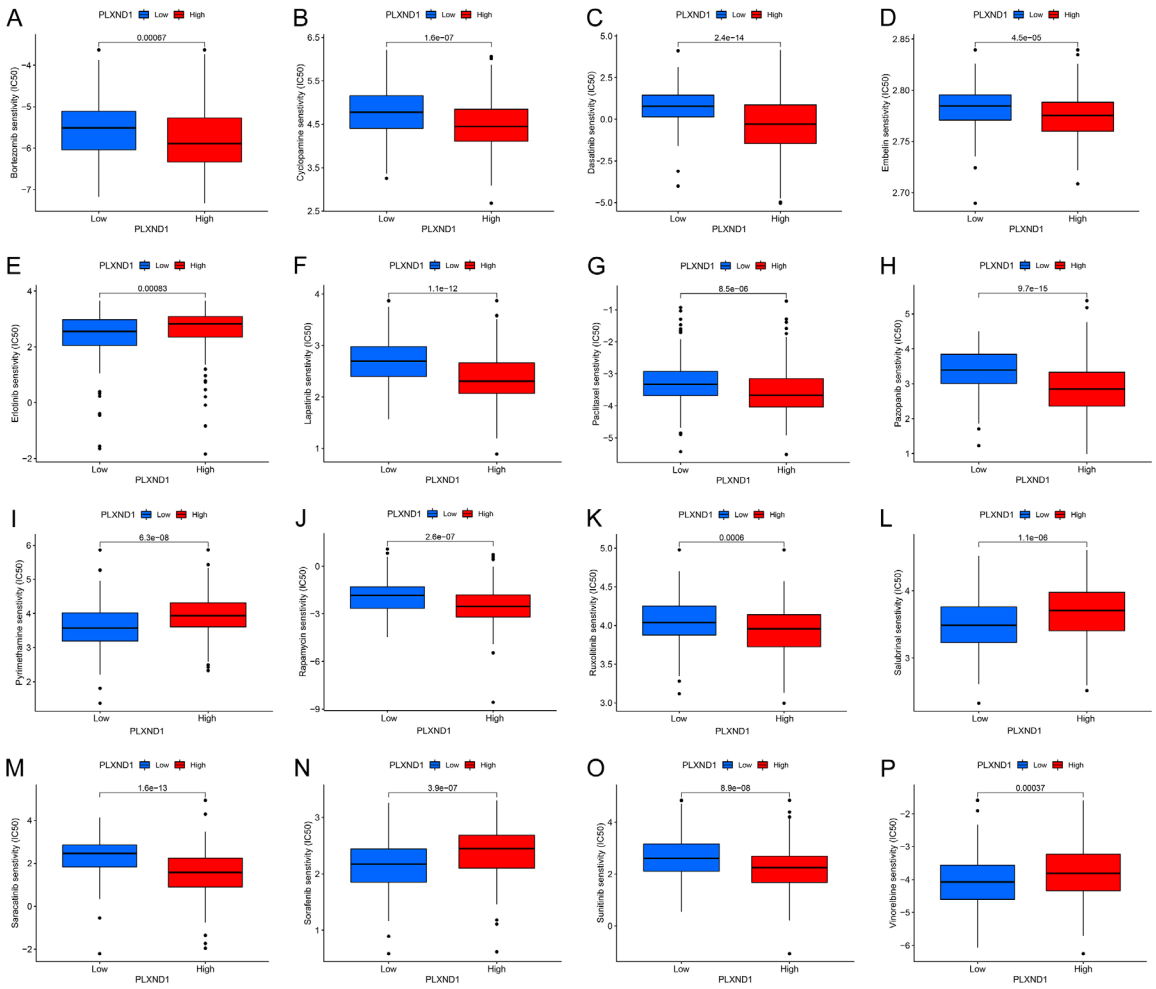

Supplementary Figure 4. Risk stratification indicated the responses of high- and low-risk groups to multiple drugs.

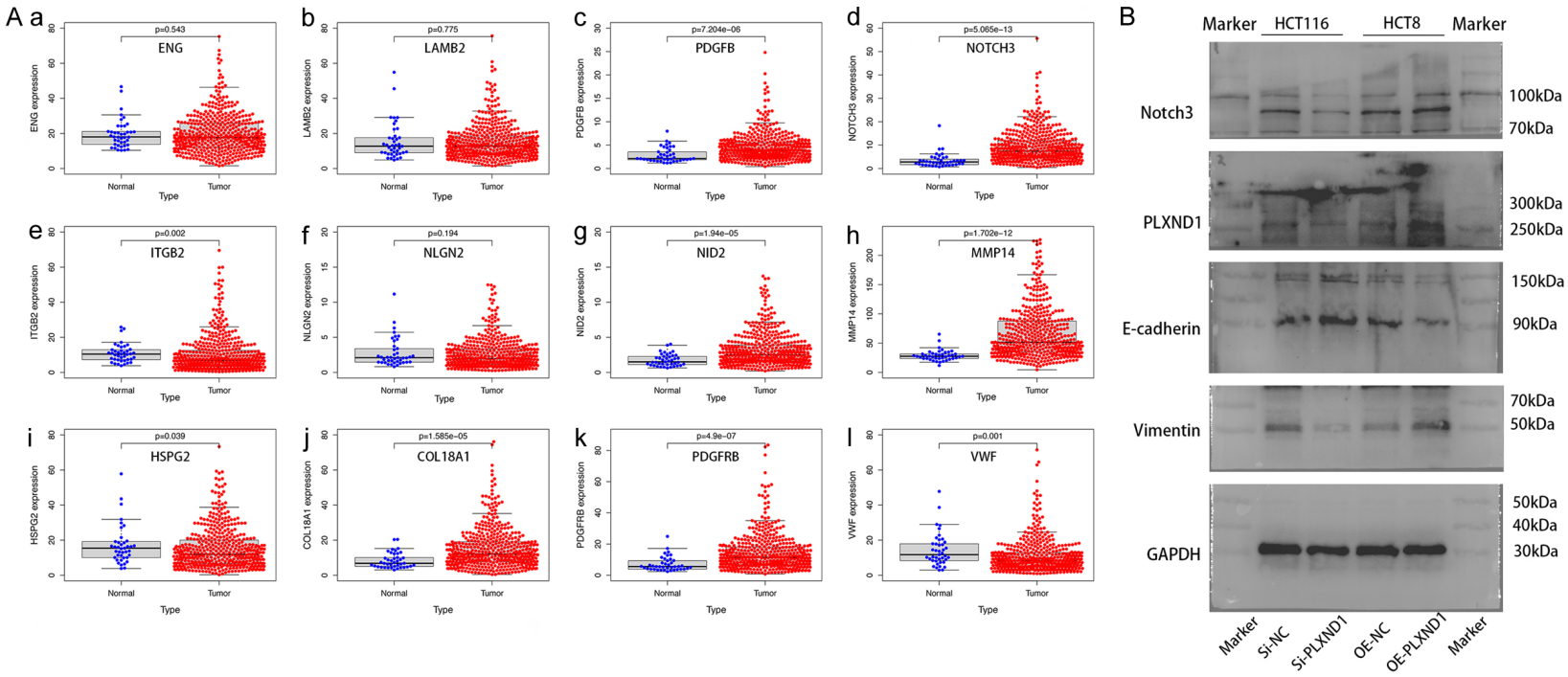

Supplementary Figure 5. A: The expression of the 12 genes was most significantly associated with PLXND1 in COAD and normal samples represented by a beeswarm. B: Plot of WB raw bands with marker.